



Review

# Flash Flood Susceptibility Modelling Using Soft Computing-Based Approaches: From Bibliometric to Meta-Data Analysis and Future Research Directions

Gilbert Hinge<sup>1</sup>, Mohamed A. Hamouda<sup>2,3</sup>  and Mohamed M. Mohamed<sup>2,3,\*</sup> 

<sup>1</sup> Department of Civil Engineering, National Institute of Technology Durgapur, Durgapur 713209, India; ghinge.ce@nitdgp.ac.in

<sup>2</sup> Department of Civil and Environmental Engineering, United Arab Emirates University, Al Ain P.O. Box 15551, United Arab Emirates; m.hamouda@uaeu.ac.ae

<sup>3</sup> National Water and Energy Center, United Arab Emirates University, Al Ain P.O. Box 15551, United Arab Emirates

\* Correspondence: m.mohamed@uaeu.ac.ae

**Abstract:** In recent years, there has been a growing interest in flood susceptibility modeling. In this study, we conducted a bibliometric analysis followed by a meta-data analysis to capture the nature and evolution of literature, intellectual structure networks, emerging themes, and knowledge gaps in flood susceptibility modeling. Relevant publications were retrieved from the Web of Science database to identify the leading authors, influential journals, and trending articles. The results of the meta-data analysis indicated that hybrid models were the most frequently used prediction models. Results of bibliometric analysis show that GIS, machine learning, statistical models, and the analytical hierarchy process were the central focuses of this research area. The analysis also revealed that slope, elevation, and distance from the river are the most commonly used factors in flood susceptibility modeling. The present study discussed the importance of the resolution of input data, the size and representation of the training sample, other lessons learned, and future research directions in this field.

**Keywords:** flash flood; bibliometric analysis; hybrid models; remote sensing; machine learning



**Citation:** Hinge, G.; Hamouda, M.A.; Mohamed, M.M. Flash Flood Susceptibility Modelling Using Soft Computing-Based Approaches: From Bibliometric to Meta-Data Analysis and Future Research Directions. *Water* **2024**, *16*, 173. <https://doi.org/10.3390/w16010173>

Academic Editors: Athanasios Loukas and Paolo Mignosa

Received: 5 October 2023

Revised: 17 November 2023

Accepted: 5 December 2023

Published: 3 January 2024



**Copyright:** © 2024 by the authors. Licensee MDPI, Basel, Switzerland. This article is an open access article distributed under the terms and conditions of the Creative Commons Attribution (CC BY) license (<https://creativecommons.org/licenses/by/4.0/>).

## 1. Introduction

Floods are considered among the most hazardous weather-related natural disasters [1], as they often severely damage natural and man-made resources [2,3]. According to statistical records from the United Nations Office for Disaster Risk Reduction (UNISDR), over 157,000 people have died between 1995 and 2015 due to several flood events, accounting for 11% of the total global disaster casualties [4]. In recent years, the occurrence rates and intensities of floods have aggravated due to climate change, as well as the increasing anthropogenic disturbance of the natural ecosystem [5,6].

The classification of floods is multifaceted, encompassing diverse dimensions that contribute to a comprehensive understanding of these natural phenomena [6]. Floods can be classified based on the source (pluvial, fluvial, coastal, groundwater), the geography of the receiving area (urban areas, river catchments, estuaries, coastal areas), the cause (excess rainfall, coastal storm events, earthquakes), and crucially, the speed of onset [7]. The speed of onset distinguishes flash floods, characterized by a rapid onset, from floods with a slower onset [8]. These characteristics impose greater challenges for predicting flash floods [8]. Therefore, accurate mapping of areas prone to flash floods is crucial for preventing loss of life and property [9]. The precise prediction of areas prone to flash floods helps not only in preparing these areas against the destructive effects of flash floods but also in harvesting floodwater, where storm floods can be diverted for human, agricultural, and livestock use [10].

Flash flood susceptibility modeling plays a critical role in creating flood-resilient communities. It involves predicting the likelihood of future flash flood events occurring

in specific areas [11]. By identifying areas with high, moderate, or low susceptibility to flash floods, it becomes possible to implement appropriate measures to prepare for and mitigate the devastating impacts of such events [12,13]. There are various approaches to flood susceptibility modeling, including physically based models and soft computing techniques. Physically based models simulate the movement of water through a system using mathematical equations that account for factors such as terrain, soil properties, and precipitation [14–17]. Hydrodynamic models are often constrained by computational limitations when it comes to large-scale applications, particularly in urban settings where a detailed depiction of intricate topographic features is necessary [14,18,19]. Soft computing techniques, also known as computational intelligence methods, are widely used in flood susceptibility modeling. These techniques include statistical models, machine learning algorithms, and other knowledge-based, data-driven approaches [20,21]. Soft computing-based techniques are now emerging as an alternative in flood susceptibility modeling and mapping, particularly in areas where flow data records are scarce. Several of these models were developed and tested in various climate and geomorphological conditions. Popular statistical methods include the frequency method [8,20] and the weight of evidence [20,22]. Among the different knowledge-based methods, the analytical hierarchy process is the most widely tested and applied [23,24]. Some popular machine learning models that are used for flash flood susceptibility modeling include artificial neural networks [25,26], random forests [27,28], and support vector machines. Recently, researchers have implemented an algorithm for a hybrid model by combining several machine-learning techniques with statistical or knowledge-based models. Ensemble machine learning techniques, such as random subspace [29,30], bagging [31], and naive Bayes [32], have gained immense popularity for achieving optimal flood-mapping performance.

Scholarly literature on flash flood susceptibility modeling using soft computing techniques has expanded substantially in recent years owing to the advancement of data acquisition techniques and the availability of a multi-model coupling approach. Therefore, it is essential to review the nature and evolution of this literature to capture conceptual and intellectual structure networks, key concepts, trends, and knowledge gaps in this field of research. Several review articles on flash floods are available in the literature [33–36], all of which focus on different aspects of flash floods. For example, Liu et al. [36] reviewed the early flash flood warning systems used in China and compared them with those used in Europe, America, and Japan. Zanchetta and Coulibaly [35] provide insights into the atmospheric conditions that preceded flash flood events. Hapuarachchi et al. [33] reviewed the advancements in remote sensing methods and their application in flash flood forecasting. Saleh et al. [34] reviewed geographic information system (GIS) integration with an empirical model for flash flood susceptibility. To the best of our knowledge, no bibliometric and meta-data analysis has investigated the origin, progression, axiomatic characteristics, and research direction of flash flood susceptibility modeling.

Different types of literature reviews are available, such as systematic literature reviews, meta-analyses, and bibliometric analyses. A meta-data analysis is a statistical technique that combines the results of multiple previous research studies to derive conclusions about that body of research [37]. Bibliometric analysis is a method that statistically analyses the scientific manuscript and its citations to draw conclusions regarding the prolificacy of authors, countries, institutions, and journals [38]. Furthermore, it helps identify research frontiers and future research gaps. Scholars from various fields, such as supply chain management [39], tsunami research [40], and social entrepreneurship, have used this method. In the field of water resources, Islam et al. [38] conducted a bibliometric analysis to review the optimum low-impact development for stormwater management practices. Dordi et al. [41] conducted a bibliometric analysis to examine the evolution of flood risk management and governance studies. Several other bibliometric studies on wastewater quality, stormwater management, and integrated water resource management are available in the literature [42,43].

This study aims to conduct a bibliometric analysis and meta-data analysis of flash flood susceptibility modeling. The following research questions were addressed:

RQ1. Which are the influential countries, key authors, and impactful and trending articles in the area of flash flood susceptibility modeling?

RQ2. How have flash flood susceptibility modeling studies evolved, and what are their key emerging research themes?

RQ3. Which algorithm/model was most commonly used, and what was its relative performance in flash flood susceptibility modeling?

RQ4. Which are the most important conditioning factors in flash flood susceptibility modeling?

This analysis will also help outline the lessons learned and the future scope of this research field.

## 2. Materials and Methods

Figure 1 shows the overall methodology adopted in this study, which comprises three main steps: (1) data extraction, (2) bibliometric analysis, and (3) meta-data analysis.

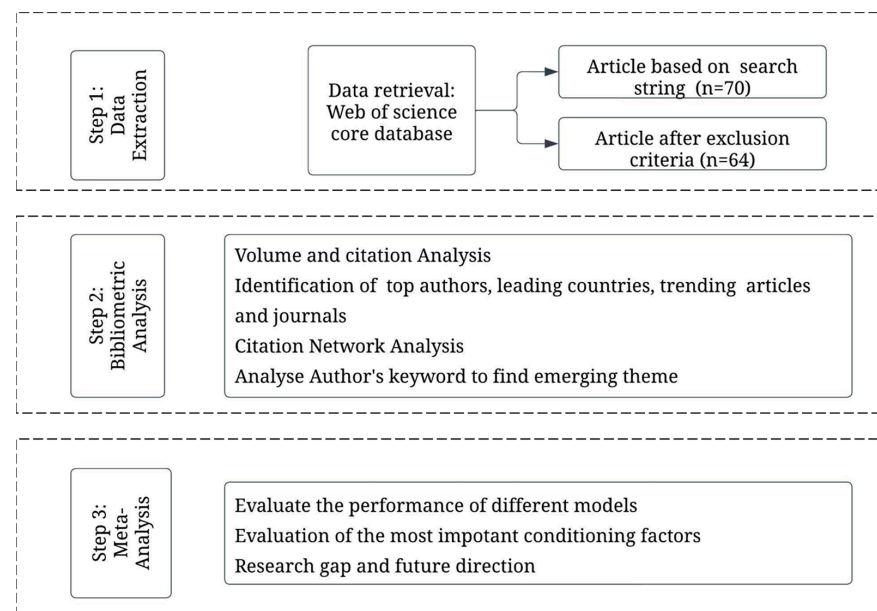


**Figure 1.** Overall Methodology.

### 2.1. Data Extraction

Articles were retrieved from the Web of Science database. We performed a Boolean search for articles on flash flood susceptibility modeling using the following combination of keywords:

("flash flood") AND ("susceptibility") AND ("modelling" OR "mapping" OR "Zoning" OR "Zonation").

The document types were limited to journal articles, and only articles written in English were included. The initial query yielded 70 articles. Furthermore, we screened the article title, abstract, and keywords and removed articles not related to flash flood or flood susceptibility modeling using soft computing techniques. This resulted in 64 articles for bibliometric and meta-data analysis. A list of all 64 articles can be found in Appendix A, Table A1.

The search criteria employed were applied to the title, abstract, and keywords of the papers. This approach was chosen to ensure a comprehensive retrieval of relevant articles while focusing on the core aspects of flood susceptibility modeling. The authors acknowledge the possibility that some articles may not explicitly include these terms in their title, abstract, or keywords. However, the selected search strategy was designed to

strike a balance between specificity and sensitivity in capturing relevant literature within the scope of our study.

## 2.2. Bibliometric Analysis

A comprehensive bibliometric analysis was performed using two software packages: HistCite (version 12.3) [44] and VosViewer (version 1.6.18) [45]. Both tools have their advantages and disadvantages. HistCite was used for bibliographic analysis, considering that it offers extensive citation analysis, while VosViewer was used for visualization, considering it has built-in graphics and algorithms.

## 2.3. Meta-Data Analysis

Essential information such as the type of prediction models, flood conditioning factors, implementation scale, and data against which the models are calibrated and validated was extracted and compiled in an Excel™ (spreadsheet 2016) spreadsheet. The top five predictors of flood conditioning factors were recorded. Information on the metric performance of various models was also extracted (Table A1). The total number of studies considered exceeded the number of articles reviewed due to the inclusion of studies that employed more than one model. Studies that used hybrid models were further classified into four categories: ML-ML, ML-O, ML-S, ML-M, and S-S. ML-ML refers to studies that include a hybrid model using ensemble machine learning approaches; ML-O refers to studies that form a hybrid model using machine learning and metaheuristic optimization algorithms; ML-S refers to studies that form a hybrid model using machine learning and statistical models; ML-M refers to studies that form hybrid models using machine learning and the multicriteria approach; and S-S refers to studies that combine two statistical models.

Different articles used different metrics, such as the probability of detection (POD) [46], false alarm ratio (FAR) [47], and area under the curve (AUC) [48], to evaluate the performance of various applied models. These metrics were evaluated at a pixel scale. However, among all the reported metrics, the area under the curve (AUC) was the most used. Hence, AUC was chosen as the metric to evaluate the performance of various categories of hybrid models. The value of AUC ranges from 0 to 1, where values close to 1 or 0 indicate the best and poorest model performance, respectively. The formulas used to determine POD, FAR, and AUC are as follows:

$$\text{POD} = \frac{TP}{TP + FN} \quad (1)$$

$$\text{FAR} = \frac{FP}{FP + TN} \quad (2)$$

$$\text{AUC} = \frac{(\sum TP + \sum TN)}{(P + N)} \quad (3)$$

where true positive ( $TP$ ) and true negative ( $TN$ ) are the numbers of correctly classified locations,  $FP$  and  $FN$  are the numbers of pixels erroneously classified by the model, and  $P$  and  $N$  are the total numbers of flooded and non-flooded locations, respectively. The importance of flash flood processes and the resolution of generated flash flood susceptibility maps vary with scale [49]. However, the classification of the study area into various spatial scales is often subjective. In this study, the extracted data on the various spatial scales were categorized into local, regional, and national scales as defined by De Moel et al. [50]. The local scale refers to a small study area of less than 100 km<sup>2</sup>. Regional scale refers to a study area of less than 100,000 km<sup>2</sup>. National scale refers to a study area larger than 100,000 km<sup>2</sup>. Information about the spatial scale for the reviewed studies was extracted and is presented in Table A1.

## 3. Results: Bibliometric

### 3.1. Trend of Publication and Citations

Figure 2 illustrates the trends in the number of publications and citations per year, starting in 2016. It is important to note that while general research on flood susceptibility

has a more extended history, this timeframe specifically pertains to recent studies within the context of flood susceptibility modeling using soft computing approaches. It was observed that the number of published articles on flash flood susceptibility modeling was very low until 2018 and showed a positive trend from 2019 onwards. Furthermore, a spike in citations was observed in the year 2020. Since no review articles were included in the analysis, the authors attributed this increase in citations to the rise in the number of articles ( $n = 18$ ) published in 2020. Moreover, we observed a decrease in the number of citations for 2021 and 2022, which could be attributed to the time taken to accumulate citations for recently published articles. Overall, the observed fluctuations in the number of publications reflect the dynamics of scholarly activities in the field of flash flood susceptibility modeling using soft computing approaches during the chosen timeframe.

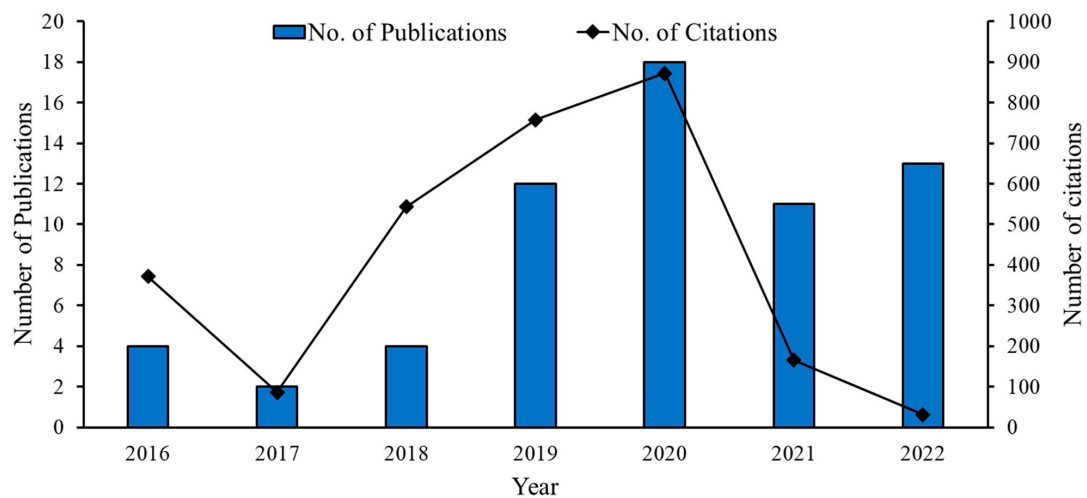


**Figure 2.** Volume and document citation by time.

### 3.2. Major Contributing Articles

The first part of the research question is to identify the major contributing articles. To observe the major articles, the top 10 articles based on total global citations (TGCS) are listed in Table 1. TGCS refers to the overall citations that the article receives from the entire Web of Science database. The total citations reported in this study are as per the Web of Science database collected as of October 2022. As per the TGCS, Khosravi et al. [51] ranked first with total citations of 321, Zhao et al. [52] ranked second with 153 citations, and Bui et al. [53] ranked third with 150 citations. Therefore, we can conclude that these three articles are the major contributing articles in flash flood susceptibility modeling. Among the recently published articles, Bui et al. [53] and Hosseini et al. [54] are the most trending articles, with a total citation of 150 and 124, respectively.

**Table 1.** Trending articles in flash flood modeling.

Sr. No.	Articles	TGCS
1	[51]	321
2	[52]	153
3	[53]	150
4	[55]	125
5	[54]	124
6	[56]	123
7	[57]	118
8	[8]	115
9	[58]	111
10	[59]	105

Note: TGCS: total global citations.

### 3.3. Contributing Authors and Their Nature of Collaboration

The second part of the first research question focuses on finding key authors and author co-citation networks based on highly cited articles. Table 2 presents the key authors in terms of the total number of global citations and publications. Based on the number of TGCS, Dieu Tien Bui was the most prominent author, contributing to 17 publications with 1172 citations. The second-most prominent author was Costache Romulus, who had 16 publications and 784 citations. The third-most prominent author was Binh Thai Pham, who had 10 publications and 725 citations. This data is as per the Web of Science database collected as of October 2022.

**Table 2.** Key authors in terms of the number of citations and publications.

Author	Numbers of Publications	TGCS
Dieu Tien Bui	17	1172
Costache Romulus	16	784
Binh Thai Pham	10	725
Phuong Thao Thi Ngo	9	565
Quoc Bao Pham	7	327
Tien Dat Pham	6	461
Alireza Arabameri	6	132
Pham Viet Hao	5	344
Nhat-Duc Hoang	4	271
Mohammadtaghi Avand	4	201

Note: TGCS: total global citations.

Figure 3 shows the authors' co-citation network. The map was generated using a minimum threshold of 30 citations, of which 16 authors met the threshold. The author's co-citation map is comprised of 16 nodes, where each node represents a different author, and the size of each node represents the co-citation strength; the greater the co-citation strength, the more prominent the node size. Furthermore, the link between a node's size indicates the extent of the collaboration. As indicated by the size and location of the nodes, Bui DT, Pham BT, Costache, Khosravi, and Tehrani are the most influential authors in this field of research. Also, it can be observed that the authors belong to different departments, such as geology, agricultural and natural research, soil conservation and watershed management, geomatics, economics, and civil engineering. This indicates that flash flood modeling draws on a wide range of knowledge and methodologies. Geologists may offer insights into the geological features and processes that contribute to flash flooding, while agricultural and natural research experts may possess knowledge of how land use and vegetation affect flood susceptibility. Meanwhile, civil engineers may contribute their expertise in infrastructure and urban planning to help mitigate flood risk, etc. Overall, this interdisciplinary collaboration among authors suggests that flash flood susceptibility modeling is a complex and multifaceted problem that requires contributions from experts in various fields.

### 3.4. Countries' Contributions and Collaboration

The third part of the first research question explored countries' contributions and collaboration patterns in this research field. Table 3 summarizes the top 10 countries ranked based on the total number of publications, global citations, and local citations. The results showed that Vietnam contributed the most to the total number of publications, followed by Iran, Romania, China, and India. Vietnam again ranked first according to TGCS, followed by Iran and India in the second and third positions, respectively. Here, the number of citations (TGCS) is associated with the total number of publications for each country in the "Number of Publications" column. Overall, the results indicate the dominance of Asian, Middle Eastern, and Western countries in the highly cited literature in this research field.

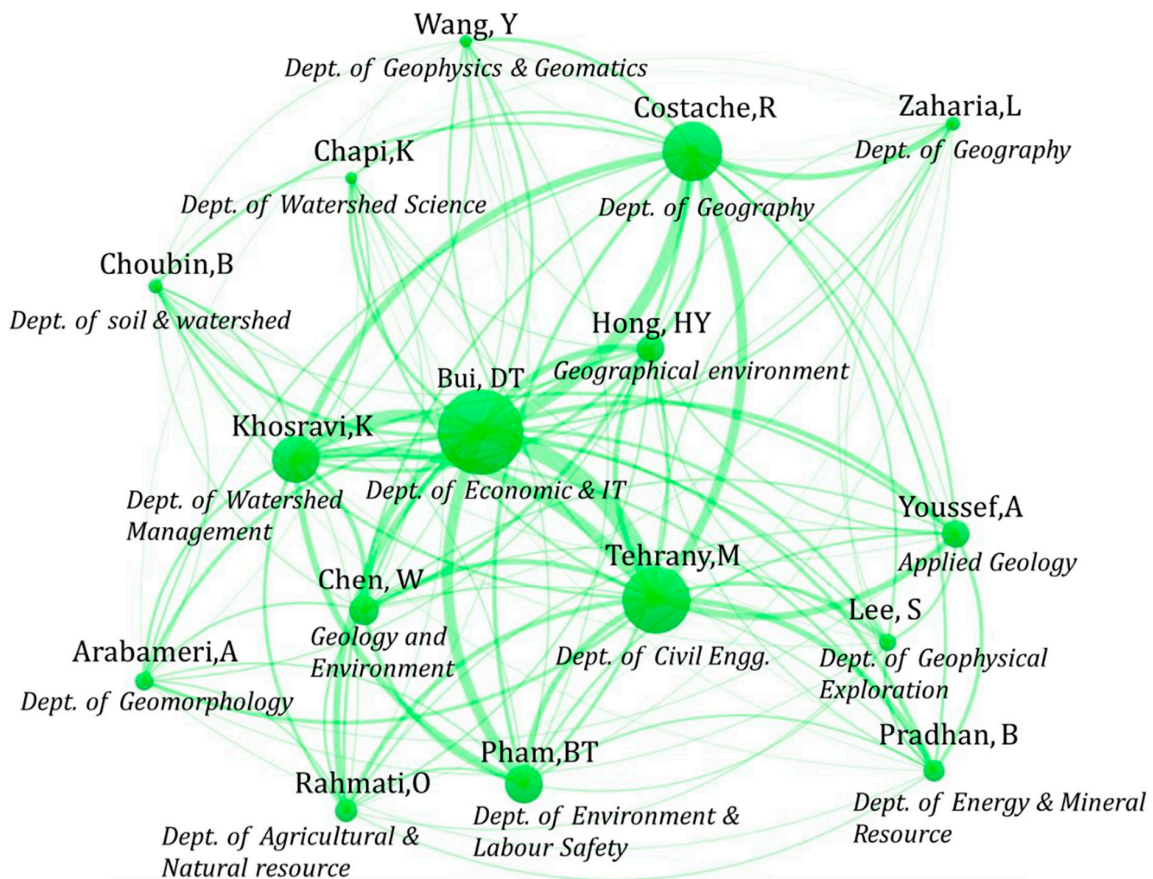


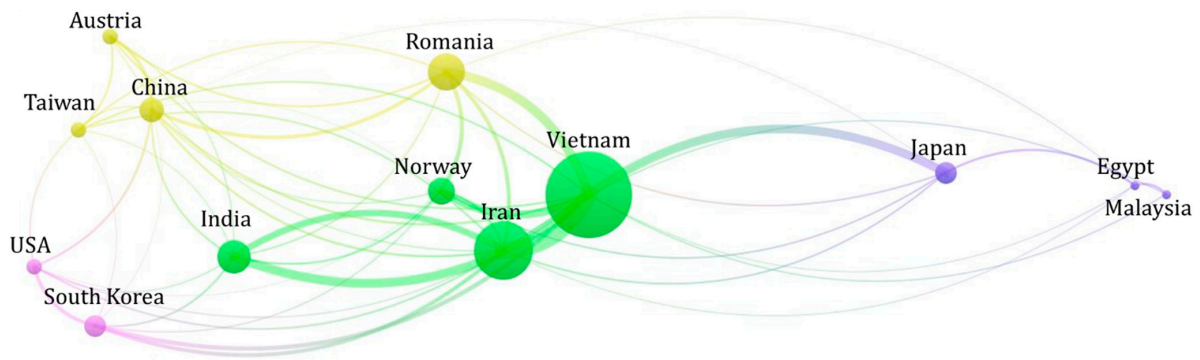
Figure 3. A network map of co-citations for different authors.

Table 3. Top ten countries based on the number of publications and citations.

Rank by Recs			Rank by TGCS		
Sr. No.	Country	Number of Publications	Sr. No.	Country	Citation Number
1	Vietnam	30	1	Vietnam	1890
2	Iran	20	2	Iran	1207
3	Romania	17	3	India	819
4	China	16	4	Romania	806
5	India	12	5	Norway	658
6	Norway	9	6	China	579
7	Japan	7	7	Japan	466
8	South Korea	7	8	USA	314
9	Austria	5	9	England	284
10	Egypt	5	10	South Korea	249

Notes: Recs: total number of publications; TGCS: total global citations.

Figure 4 shows the country collaboration network based on the top papers (in terms of citations) on flood susceptibility modeling. The map was generated using a minimum threshold of five documents from a country; 13 countries met this criterion. As seen in the figure, Vietnam and Iran collaborated with 12 countries, representing the maximum collaboration among countries, with a total link strength of 28 and 19, respectively. This could be the reason why Vietnam had the most cited articles. China collaborated with ten countries for a total link strength of eight. India and Norway collaborated with nine countries. These findings indicate the importance of international collaboration in producing highly cited articles, agreeing with the results of other authors, who reported a positive correlation between highly cited articles and international collaboration [60].



**Figure 4.** A network map of co-authorship and country.

3.5. Emerging Theme

The second research question focused on key emerging themes and their evolution. The authors’ keywords were used to evaluate emerging research themes. A keyword is considered the most common emerging keyword if it appears at least ten times in all titles and abstracts. Of the total keywords, 16 met this threshold. Among these 16, keywords such as flood, floods, flash flood, flash floods, flash-floods, vulnerability, hazard, flood hazard, flood mapping, flood risk, flood risk management, flood susceptibility, and risk assessment were eliminated, resulting in 8 keywords, as shown in Table 4. Among these, “Frequency ratio” and “GIS” are the most recurrent keywords, with 27 and 25 occurrences, respectively. Figure 5 shows these eight keywords, where each node represents a keyword, and the size of each node represents the number of occurrences of keywords.

**Table 4.** Top keyword based on the number of occurrences.

Keyword	Occurrence
Frequency Ratio	27
GIS	25
Logistic Regression	24
Weight of Evidence	20
Statistical Models	14
Support Vector Machine	12
Analytical Hierarchical Process	10
Machine Learning	10

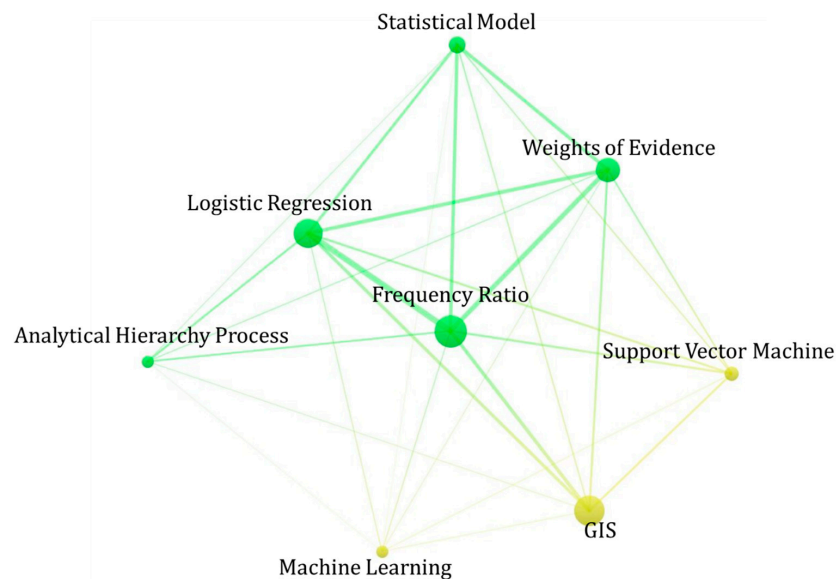


**Figure 5.** Emerging theme based on the author’s keyword network.



## 4. Results: Meta-Analysis

### 4.1. Frequency and Comparative Performance of Algorithms for Flash Flood

It was found that various techniques, ranging from standard machine learning or multicriteria to advanced and hybrid models, were applied for flash flood susceptibility mapping (refer to Table A1).

Figure 6 shows the frequency of applied algorithms for flash flood modeling. It was observed that most studies implemented hybrid algorithms by combining several machine learning techniques with statistical models, knowledge-based models, or metaheuristic optimization algorithms. Of the 64 articles, 38 articles used hybrid models. This was followed by articles that used standalone machine learning or statistical or knowledge-based models such as neural networks, frequency ratios, analytical hierarchy processes, support vector machines, etc. Figure 6 also shows the number of articles that compare different algorithms and those where a particular algorithm was found to be better than the others. Overall, the hybrid models performed better than the standalone and standard models, except for the study by Youssef et al. [59], where the standalone frequency ratio model performed better than the ensemble frequency ratio and logistic regression. As shown in Figure 6, all the standard standalone models performed poorly in the comparative studies, considering all the articles comparing standalone models and hybrid models.

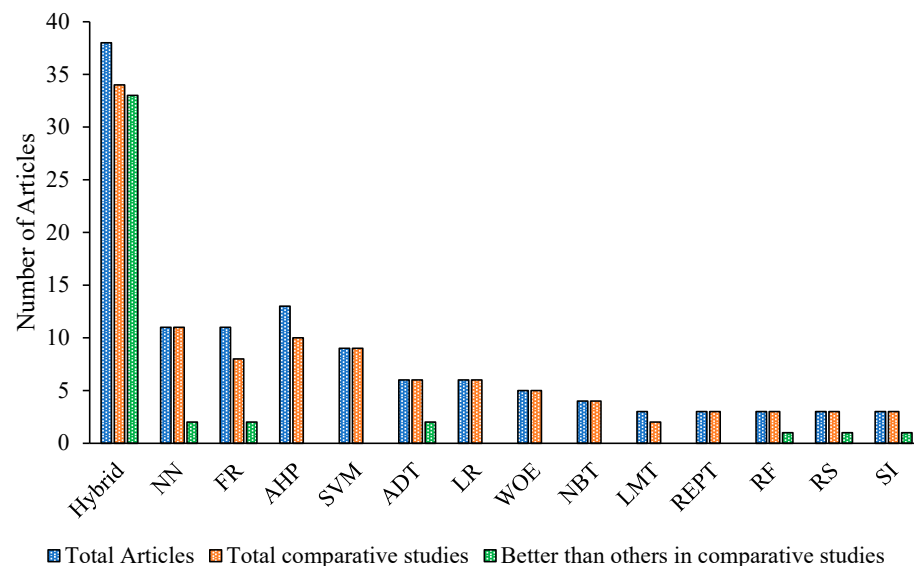


**Figure 6.** Frequency of use and comparative performance of algorithms for flash flood susceptibility modeling (NN: Neural Network, FR: Frequency Ratio, AHP: Analytical Hierarchical Process, SVM: Support Vector Machine, ADT: Alternating Decision Trees, LR: Logistic Regression, WOE: Weight of Evidence, NBT: Naïve Bayes Trees, LMT: Logistic Model Trees, REPT: Reduced Error Pruning Trees, RF: Random Forest, RS: Random Subspace, SI: Statistical Index).

### 4.2. Performance of Various Hybrid Models

Given the superior performance of hybrid models over standard or standalone models, this study further classified the hybrid models into different categories, as described in the methodology section, to guide the selection of the most effective hybrid models. Figure 7 shows the mean AUC values that indicate the impact of the hybrid model selection on the performance of flash flood prediction. The availability of advanced machine learning approaches, such as extreme learning machines, multilayer perceptron neural networks, and deep learning neural networks, has led to the wide application of coupled machine learning techniques or, in some cases, the output of various machine learning models being combined to form hybrid models (Figure 7). Additionally, several studies have attempted to weigh flash flood predictors from a statistical point of view or based on expert judgment. These weights are then used as inputs for machine learning to form a hybrid model.

Among all hybrid models, ML-O was found to have the best performance (AUC = 0.96), followed by ML-S (AUC = 0.94), ML-ML (AUC = 0.93), ML-M (AUC = 0.93), and S-S (AUC = 0.89). However, it is crucial to emphasize that while mean AUC values provide valuable performance benchmarks, the study recognizes the paramount importance of accounting for the standard error associated with these models. This underscores the need for a nuanced consideration of context-specific factors when making informed decisions about model selection. Furthermore, it is worth noting that the studies considered in this analysis encompassed diverse geographical regions around the world (Table A1). The quality and quantity of available data, as well as computational resources, varied across these regions, further emphasizing the need for adaptable and context-aware flood susceptibility modeling approaches.

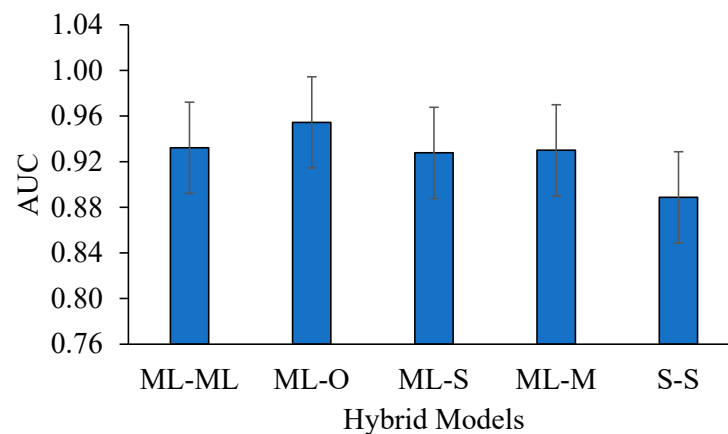


**Figure 7.** Performance evaluation of different hybrid models (ML-ML: Machine Learning–Machine Learning, ML-O: Machine Learning–Optimization Technique, ML-S: Machine Learning–Statistical Model, ML-M: Machine Learning–Multicriteria, S-S: Statistical–Statistical).

#### 4.3. Important Flash Flood Conditioning Factors

Figure 8 shows the frequency of usage of the most important flash flood conditioning factors for flash flood susceptibility modeling. The five most important conditioning factors were considered for each of the 64 articles listed in Table A1. The slope was ranked 37 times as the most important factor, followed by elevation (25 times), distance from a river (21 times), land use and land cover (19 times), curvature (17 times), and lithology (14 times).

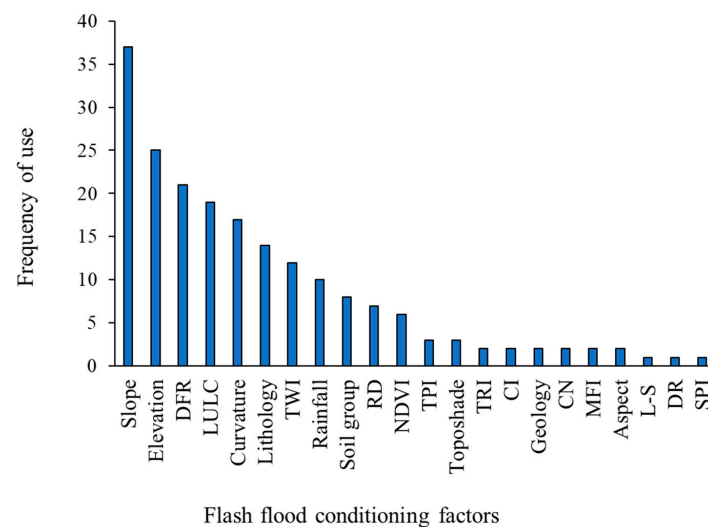


**Figure 8.** Frequency of the most important flash flood conditioning factors (LULC: Land Use Land Cover; TWI: Topographic Wetness Index; DFR: Distance From River; RD: Drainage Density; NDVI: Normalized

Difference Vegetation Index; TPI: Topographic Position Index; TRI: Topographic Roughness Index; CI: Convergence Index; CN: Curve Number; MFI: Modified Fourier Index; L-S: Length and Steepness Factor; DR: Distance to Road; SPI: Stream Power Index).

## 5. Discussion

### 5.1. Bibliometric Analysis

Studies on flash flood susceptibility modeling using soft computing techniques have increased substantially in recent years, thereby providing a research opportunity on the developments in this field. Related articles were retrieved from the Web of Science database to conduct this review. First, the publication trends of articles in terms of the volume of documents and number of citations were generated. An increasing trend was observed in terms of the number of published articles in 2019, which indicated that the topic remains relevant to the emerging concept. One of the possible reasons for the increase in the number of publications and citations in recent years is the increase in the frequency and intensity of flash floods [61]. Therefore, in recent years, scientists worldwide have attempted to model and map areas affected by flash floods to prepare against and mitigate the devastating impact of such events in the future.

Next, citation analysis was conducted in terms of local and global citations to identify the trending articles in this research field. It is worth noting that the top 10 most-cited articles in this field primarily focused on flash floods occurring in mountainous catchments or river catchments, denoting the importance of such locations in terms of flash flood occurrences. In addition, most of these studies used remotely sensed imagery as the input to flash flood models, indicating that remote sensing data have increased tremendously in this field [9].

A collaboration analysis was conducted to determine the nature of the collaboration between the authors and the countries. Additionally, a country network map was generated, which showed that Vietnam led the chart in terms of the number of publications and had the highest number of citations. Interestingly, it was found that countries with the highest collaboration were associated with more citations (Table 4), which indicated the importance of collaboration among countries from various regions when publishing highly cited articles in a specific field. The study also evaluated emerging themes based on the author's keywords. Among the author's keywords, GIS, statistical model, frequency model, machine learning, and multicriteria analysis were the most commonly used keywords, thereby laying out the key future research themes in this research area.

### 5.2. Meta-Data Analysis

Owing to the rapid advancement of innovative technologies, various hybrid models have been developed and applied to flash flood modeling. These hybrid models were found to perform better than standard models in most cases. Remote sensing data played a vital role in the performance of flood susceptibility models, considering remote sensing helps generate diverse flash flood predictors [62]. Remote sensing is a valuable source of data that may complement and, in some cases, replace field surveys, particularly in remote areas and ungauged basins [63]. The availability of remote sensing data could help trace the areas affected by flash flood events. Utilizing various remote sensing data also helps develop digital elevation models, land use and land cover, inundation extent, water level, river width, topography, geology, and several other attributes that shed light on the causes of flash flood events and enhance the prediction of future events. With forthcoming satellite missions such as the Surface Water and Ocean Topography (SWOT) mission [64] and high temporal and spatial resolution satellites such as Sentinel 2, PlanetScope, etc., remote sensing will play a significant role in enhancing our capability in understanding and predicting flash floods.

On comparing the standard models, in many cases, the machine learning model exhibited higher prediction accuracy than the expert-based methods. For example, Nachappa et al. [2] found that the standalone random forest and support vector machine outperformed the analytic hierarchy and analytic network processes. Machine learning methods, such

as naive Bayes, are superior to knowledge-based learning methods, such as Technique for Order of Preference by Similarity to Ideal Solution (TOPSIS) and Vlekkriterijumsko Kompromisno Rangiranje (VIKOR) [65]. Among the machine learning models, Khosravi et al. [51] compared the performance of logistic model trees, reduced error pruning trees, naive Bayes trees, and alternating decision trees (ADT) and found that ADT performed better than the other models. Similarly, Bui et al. [53] compared the performance of advanced machine learning, such as deep learning neural networks (DLNN), multilayer perceptron neural networks, and support vector machines, and found that DLNN outperformed the other models. However, knowledge-based methods also provided excellent flash flood hazard mapping results at many locations [23,62]. In addition, techniques such as frequency ratio, the weight of evidence, and the statistical index reportedly had superior accuracy at many locations [66]. The results show that there is no single best standalone model for flash flood susceptibility. Therefore, researchers worldwide have considered two or more ensemble methods to take advantage of the merits of each and form a hybrid model with better prediction performance [51]. This is evident in Figure 6, which shows that the hybrid models performed better than the standalone models.

Although hybrid models have several advantages, optimizing the model parameters is a challenge that can often lead to overlearning of the model, particularly in machine learning [56]. Therefore, coupling the machine learning approach with metaheuristic optimization algorithms could help achieve better prediction performance compared to other hybrid models [30]. This is because optimization algorithms first search for the best input parameters and optimize the layers' weights [56]. This is evident in Figure 7, which shows that the hybrid model that combines the machine learning approach with the heuristic optimization technique exhibited better overall performance, with AUC values of 0.96. However, it is worth noting that the performance of all hybrid models, barring S-S, is greater than 0.93 (in terms of AUC). However, as the performance of the models may be influenced by the sample size, basin characteristics, climate type, and number of training and testing datasets, more comparative studies of hybrid models in the same research area should be conducted to make explicit judgments about their performance. As seen from Table A1, the majority of the reviewed studies have considered a regional scale equivalent to a province, catchment, or big city. Five papers [52,67–70] have carried out flash flood modeling at national scales. Even though few of the reviewed studies do not encompass an entire nation, they were categorized as national-scale studies because the area of investigation was more than 100,000 km<sup>2</sup>. Interestingly, only one study [8] was carried out on a local scale. With the availability of high computation power and remote sensing data at various temporal and spatial scales, more future studies are expected to investigate flash flood susceptibility modeling at both national and local scales.

This study also evaluated the frequency of use of the most important flash flood conditioning factors, which include those directly or indirectly associated with the occurrence of flash floods [71]. As satellite and remotely sensed information increase, various factors related to soil type, topography, vegetation, and climate are used to optimize the prediction of flash flood locations [61]. From the analysis, the top six most important conditioning factors were slope, elevation, distance to a river, LULC and curvature, and topographic wetness index. The slope is a measure of the degree of steepness of a location and is directly related to surface runoff, thereby influencing flash flooding. Areas with milder slopes are prone to flash floods, as these areas are the first to flood during flash flood events [72]. Similarly, lower-elevation areas are susceptible to flash floods as flood water flows from higher to lower elevations [73]. LULC is another crucial factor influencing infiltration and surface runoff generation and is directly related to flash floods. The increase in the magnitude and frequency of flash floods is often related to changes in land use and land cover [74]. The major changes in LULC that affect flash floods are deforestation, intensive agriculture, and the conversion of natural landscapes into impervious man-made structures. Curvature, which indicates the rate of change in the slope gradient in a particular direction, is another influential factor in flash floods [75]. Positive and negative curvatures indicate that the

slope gradient is convex and concave in the upward direction, respectively, whereas a zero value indicates a flat curvature. Usually, areas with a flat curvature are highly susceptible to flash floods [76]. The topographic wetness index indicates the topographic control over the hydrology of an area. Based on this index, one can estimate where the flood water would accumulate while considering the elevation differences [73]. Given that TWI shows the wetness of an area, areas with higher TWI are likely to have saturated soil, leading to a higher potential for flash flood occurrence [77].

## 6. Limitations of This Study

This study considered the top ten articles, countries, and authors for ranking. In addition, a higher threshold was set to generate network maps of authors and countries and evaluate the emerging themes in this research field. These thresholds were selected to be able to present a clear and readable visualization of collaborations and emerging themes. However, as the remaining articles were not considered, the nature of collaboration between authors and the countries with fewer publications and citations was not shown. Moreover, this study conducted a meta-data analysis to answer only a few major questions. Future studies could tailor more meta-data analysis to answer other relevant research questions, such as the impact of implementation scale, topography, climatic conditions, and basin characteristics on the performance of the model.

Also, the present study only considers articles that used soft computing techniques for Flood susceptibility mapping. A common limitation identified across multiple studies is the dependency on data-driven algorithms in soft computing models. While these algorithms showcase notable predictive capabilities, they may fall short of fully capturing the underlying physical processes governing flash floods [78]. As a result, the susceptibility models developed based on these approaches might encounter inaccuracies, particularly in areas characterized by complex or unique terrain features. In such cases, physically based models governed by physical laws and equations may be better suited [14]. However, it is worth noting that physically based models can also have their limitations, such as high computational requirements and the need for detailed and accurate input data. Therefore, future studies should compare the strengths and weaknesses of these models and determine which would be best suited for different scenarios.

## 7. Conclusions

In recent years, the frequency of flash floods has increased. In response, scholarly articles in this field have grown exponentially. In this study, we conducted a bibliometric analysis and meta-data analysis of flash flood susceptibility modeling. Furthermore, we summarised the state of the art of development in this field to help researchers, geohazard scientists, and decision-makers working in this field. The key conclusions drawn from this review are as follows:

- (a) The publication trend graph indicated that the publication of articles in this research field started in 2016 and has increased since 2019.
- (b) Citation analysis indicated that papers titled "A comparative assessment of decision tree algorithms for flash flood susceptibility modeling at Haraz watershed, northern Iran" had the highest number of citations as per the Web of Science database collected as of October 2022.
- (c) The author's keyword analysis showed that GIS, machine learning, statistical models, and analytical hierarchy processes were the central focuses of this research area.
- (d) The hybrid models performed better than the standalone models. Models combining metaheuristic optimization algorithms and machine-learning approaches performed better than other hybrid models.

Based on the above findings, the following recommendations can be adopted for future studies:

- (a) Factors affecting flash floods may differ depending on climatic conditions and basin characteristics. Therefore, future studies should review the most important factors by

characterizing the study areas concerning climate conditions and basin characteristics. More comparative studies of hybrid models in the same research area should be conducted to judge their performance explicitly.

- (b) While choosing better models and conditioning factors is essential for improving prediction performance, other aspects, such as the size and representation of training samples, are equally important for assessing the performance of flash flood susceptibility models.
- (c) The impact of input dataset resolution on the model's performance has not been extensively explored. Therefore, future studies should explore the impact of the resolution of the input data on the outcome of flash flood susceptibility maps.
- (d) A critical reflection of the transferability of flash flood susceptibility models is necessary. Hence, future studies should explore the validity of transferring the developed flash flood susceptibility model and evaluate its performance using new data from another region. However, before transferring the model to a new region, it is essential to carefully evaluate its similarities and differences. It is also recommended to use a robust statistical method to validate the model's performance on new data from other regions to ensure reliability and accuracy.
- (e) Future studies should also compare the output of the flash flood susceptibility model obtained using computing-based techniques with the physically based model output to identify the strengths and weaknesses of each approach and determine which is better suited for different applications and scenarios.

**Author Contributions:** Conceptualization, G.H., M.A.H. and M.M.M.; data curation, G.H. and M.A.H.; formal analysis, G.H.; funding acquisition, M.M.M. and M.A.H.; investigation, G.H.; methodology, G.H.; project administration, M.A.H. and M.M.M.; resources, M.M.M. and M.A.H.; supervision, M.A.H. and M.M.M.; validation, M.A.H.; visualization, G.H.; writing—original draft preparation, G.H.; writing—review and editing, M.A.H. and M.M.M. All authors have read and agreed to the published version of the manuscript.

**Funding:** This research was funded by the National Water and Energy Center, United Arab Emirates University, through the Asian University Alliance (AUA) program, grant number 12R176-AUA-NWEC-4-2023.

**Data Availability Statement:** The data that support the findings of this study are available from the corresponding author upon reasonable request.

**Conflicts of Interest:** The authors declare no conflict of interest.

## Appendix A

**Table A1.** Referred articles for systematic review (Logistic Model Trees: LMT, Reduced Error Pruning Trees: REPT, Naïve Bayes Trees: NBT, Alternating Decision Trees: ADT, Analytical Hierarchical Process: AHP, Feed-Forward Neural Networks: BP, Genetic Algorithm: GA, Multilayer Perceptron: MLP, Bayesian Belief Network: BN, Shuffled Frog-Leaping Algorithm: SFLA, Artificial Neural Network: ANN, Support Vector Machine: SVM, Random Forest: RF, Random Subspace: RS, Dagging Ensemble Model: DAE, Index of Entropy: IOE, Fuzzy Unordered Rules Induction Algorithm: FURIA, Firefly algorithm: FA, Levenberg–Marquardt Backpropagation: LM, Classification Tree: CT, FR: Frequency Ratio, LR: Logistic Regression, Functional Tree: FT, Bagging-Functional Tree: BFT, Dagging-Functional Tree: DFT, Rotational Forest-Functional Tree: RFT, Reduced Error Pruning trees: REPT, Extreme Learning Machine: ELM, Particle Swarm Optimization: PSO, Quantum Particle Swarm Optimization: QPSO, Credal Decision Tree: CDTree, Statistical index: SI, Boosted Regression Tree: BRT, Naive Bayes Tree: NBT, Boosted Generalized Linear Model: GLMBoost, Bayesian Generalized Linear Model: BayesGLM, Lazy K-Star: KS, k-Nearest Neighbor: kNN, Convolutional Neural Network: CNN, Fuzzy Membership Value: FMV, Evidential Belief Function: EBF, Random Subspace: RS, MultiBoosting: MJ, Real AdaBoost RAb, Kernel Logistic Regression: KLR, Quadratic Discriminant Analysis: QDA, Weights of Evidence: WOE, Firefly Particle Swarm Optimization: HFPS, Random Subspace Tree: RSTree, Shannon’s Entropy: SE, Weighing Factor: Wf, Multivariate Adaptive Regression Splines: MARS, Particle Swarm Optimization: PSO, Recurrent Neural Networks: RNN, AdaBoostM1 Based Credal Decision Tree: ABM-CDT, Bagging Based Credal Decision Tree: Bag-CDT, Dagging based Credal Decision Tree: Dag-CDT, MultiBoostAB based Credal Decision Tree: MBAB-CDT, Single Credal Decision Tree: CDT, Deep Belief Network with Back Propagation Algorithm Optimized by the Genetic Algorithm: DBPGA, Adaptive Neuro-Fuzzy Inference System: ANFIS).

References	Model Used (Best Model in Bold)	Study Area	Top 5 Predictors Reported (in No Order)	Implementation Scale	Resolution of the Map Generated	Performance of Models (Based on AUC)	Data against Which the Model Are Validated
[51]	LMT, REPT, NBT, <b>ADT</b>	Iran	Ground slope, altitude, Topographic Wetness Index (TWI), river density, distance from river.	Regional (4014 km <sup>2</sup> )	-	ADT-0.976 NBT-0.974 LMT-0.971 REPT-0.811	Past field survey data
[52]	<b>RF</b> , ANN, SVM	China	Elevation, longitude, drainage density, soil moisture, average annual daily maximum Precipitation	National (4,280,000 km <sup>2</sup> )	11.1 × 11.1 km	RF: 0.838	Historical flooding record
[53]	<b>DLNN</b> , MLP-NN, SVM	Vietnam	Elevation, slope, curvature, soil type, lithology	Regional (1465.07 km <sup>2</sup> )	-	DLNN-0.960	Past field survey data
[55]	SE, <b>SI</b> , Wf	Iran	Distance from River, Rainfall, Geology Land use, NDVI	Regional (4015 km <sup>2</sup> ).	20 × 20 m	SE-0.914 SI-0.987 Wf-0.976	Documentary source and field data
[65]	<b>NBT</b> , NB, SAW, TOPSIS, VIKOR	China	Elevation, distance from river, NDVI, soil type, Slope	Regional (4053.16 km <sup>2</sup> ).	-	NBT-0.984 NB-0.979 SAW-0.97 TOPSIS-0.968 VIKOR-0.965	Past field survey data

Table A1. Cont.

References	Model Used (Best Model in Bold)	Study Area	Top 5 Predictors Reported (in No Order)	Implementation Scale	Resolution of the Map Generated	Performance of Models (Based on AUC)	Data against Which the Model Are Validated
[54]	GLMBoost, BayesGLM, <b>RF</b>	Iran	Elevation, drainage density (Dd), distance from stream (Dfs), normalized difference vegetation index (NDVI)land use	Regional (11,290 km <sup>2</sup> )	30 × 30 m	-	Inundation map generated from Sentinel 2 images
[56]	<b>PSO-ELM</b> , MLP-ANN, SVM, Decision Tree	Vietnam	Elevation, slope, aspect, curvature, Toposhade,	Regional (1510.4 km <sup>2</sup> )	20 × 20 m	PSO-ELM- 0.954 MLP-ANN-0.938 SVM-0.93 Decision Tree-0.912	Past field survey data
[7]	<b>PSO-MARS</b> , BNN, SVM, CT	Vietnam	Elevation, slope, toposhade, aspect, topographic wetness index	Regional (1510.4 km <sup>2</sup> )	10 × 10 m	PSO-MARS: 0.96	Historical record
[57]	<b>FURIA-GA-Bagging</b> ; FURIA-GA-LogitBoost; FURIA-GA-AdaBoost	Vietnam	Elevation, slope, topographic wetness index (TWI), toposhade, lithology cover	Regional (1510 km <sup>2</sup> )	-	FURIA-GA-bagging: 0.9540 FURIA-GA-LogitBoost: 0.8330 FURIA-GA-AdaBoost: 0.9520	Field Survey
[79]	<b>RF-ADTree</b> SVM-Polynomial, SVM-RVF, LR, AD-Tree, NBMU	Iran	Distance to river, geomorphology, Landsuse, HG, Geology, Slope	Regional (489.49 km <sup>2</sup> )	-	RF-ADTree-0.906 SVM-Polynomial-0.879 SVM-RVF-0.867 LR-0.75 AD-Tree-0.861 NBMU-0.811	Field Survey, Past data
[71]	<b>DBPGA</b> , LR, LMT, ADT, NBT, ANFIS-BAT, ANFIS-CA, ANFIS-IWO, ANFIS-ICA, ANFIS-FA	Iran	No ranking	Regional (4014 km <sup>2</sup> )	-	DBPGA: 0.989 ANFIS-BAT: 0.944 ANFIS-CA: 0.921 ANFIS-IWO: 0.939 ANFIS-ICA: 0.947 ANFIS-FA: 0.917	Historical record
[8]	<b>FR</b> , SI	China	No ranking	Local (7.98 km <sup>2</sup> )	-	-	Documentary source and field data
[58]	ANN, SVM, RF, RS, <b>Dagging</b>	Bangladesh	Slope, topographic roughness index (TRI), elevation, LULC, distance to road	Regional (2284 km <sup>2</sup> )	30 × 30 m	Dagging-0.873 SVM-0.86 ANN-0.83 RF-0.91	Historical data sources, fieldwork, perception of local residents, and Google Earth



Table A1. Cont.

References	Model Used (Best Model in Bold)	Study Area	Top 5 Predictors Reported (in No Order)	Implementation Scale	Resolution of the Map Generated	Performance of Models (Based on AUC)	Data against Which the Model Are Validated
[59]	<b>FR</b> ; FR+LR	Saudi Arabia	Slope, Elevation, Curvature, Geology, Land use	Regional (219 km <sup>2</sup> )	5 × 5 m	FR-0.896 FR-LR: 0.913	Field survey
[80]	<b>ADT</b> , FT, KLR, MLP, QDA	Iran	Elevation, slope, distance from rivers, land use, lithology	Regional (1605 km <sup>2</sup> )	-	-	Historical flood map
[81]	<b>kNN-AHP</b> , KS-AHP, KS, KNN	Romania	Slope angle, profile curvature, curve number, lithology, modified Fournier index	Regional (2600 km <sup>2</sup> )	30 × 30 m	kNN-AHP: 0.901 KS-AHP: 0.886	Remote sensing images and field survey
[82]	<b>DNN-GWO</b> , DNN-GOA, <b>DNN-SSO</b> ,	Vietnam	NDVI, distance to river, aspect, slope, NDBI	-	30 × 30 m	DNN-GWO: 0.96 DNN-GOA: 0.96 DNN-SSO: 0.97	Sentinel-1A images in combination with field surveys
[83]	<b>ABM-CDT</b> , Bag-CDT, Dag-CDT, MBAB-CDT CDT	Iran	Distance from rivers, elevation, slope, soil, lithology.	Regional (1605 km <sup>2</sup> )	12.5 × 12.5 m	ABM-CDT: 0.957 Dag-CDT: 0.947 MBAB-CDT: 0.933 Bag-CDT: 0.932	Historical record
[84]	<b>LR-FR</b> , LR-WoE, SVM-FR, SVM-WoE	Romania	Slope angle, land use, lithology, plan curvature, and profile curvature	Regional (2600 km <sup>2</sup> )	30 × 30 m	LR-FR: 0.888 LR-WOE: 0.885 SVM-FR: 0.887 SVM-WOE: 0.883	Orthorectified aerial imagery and field survey
[73]	MLP-FR, MLP-WOE, <b>RF-FR</b> , RF-WOE	Romania	Slope angle, LULC, distance from river, rainfall, stream power index	Regional (2509 km <sup>2</sup> )	-	MLP-FR: 0.940 MLP-WOE: 0.946 RF-FR: 0.999 RF-WOE: 0.968 CART-WOE: 0.938 CART-FR: 0.937	Historical record
[74]	<b>FA-LM-ANN</b> ; LM-ANN; FA-ANN-SVM; CT	Vietnam	No ranking	Regional (1510.4 km <sup>2</sup> )	-	FA-LM-ANN: 0.985 LM-ANN: 0.957 FA-ANN: 0.972	Sentinel-1A SAR imagery
[85]	AHP, IAE, <b>ADT-IOE</b> , ADT-AHP	Romania	Slope angle, topographic position index, plan curvature, land use, convergence index	Regional (363 km <sup>2</sup> )	-	ADT-IOE: 0.972 ADT-AHP: 0.926	Google Earth aerial imagery
[86]	<b>BRT</b> , <b>ERT</b> , PRF, RF, RRF	Iran	Altitude, slope, aspect, Plan curvature, profile curvature	Regional (2056.75 km <sup>2</sup> )	-	BRT: 0.75 ERT: 0.82 PRF: 0.79 RF: 0.78 RRF: 0.80	Field survey and local authority

Table A1. Cont.

References	Model Used (Best Model in Bold)	Study Area	Top 5 Predictors Reported (in No Order)	Implementation Scale	Resolution of the Map Generated	Performance of Models (Based on AUC)	Data against Which the Model Are Validated
[87]	SI, LR-SI, CART-SI, <b>MLP-SI</b> , RF-SI, SVM-SI	Romania	Slope relief, L-S Factor, Topographic Wetness Index (TWI), profile curvature and Topographic Position Index (TPI), land use	Regional (340 km <sup>2</sup> )	30 × 30 m	LR-SI: 0.915 CART-SI: 0.929 MLP-SI: 0.942 RF-SI: 0.903 SVM-SI: 0.894	Aerial imagery and field measurements
[22]	LMT, RF, ADT, WoE, LMT-WoE, RF-WoE, <b>ADT-WoE</b>	Romania	Slope, profile curvature, curve number, lithology, modified Fournier index	Regional (2600 km <sup>2</sup> )	30 × 30 m	LMT-WoE: 0.906 RF-WoE: 0.893 ADT-WoE: 0.917	Aerial Imagery and field survey
[88]	<b>RS</b> , MJ, RAb	Iran	Elevation, stream distance, precipitation, land use/land cover (LU/LC), normalized difference vegetation index (NDVI)	Regional (11,290 km <sup>2</sup> )	-	RS: 0.931 MJ: 0.901 RAb: 0.889	Historical record and field survey
[89]	FT, <b>BFT</b> , DFT, RFT	Iran	Elevation, Drainage density, distance to stream, rainfall, NDVI	Regional (11,290 km <sup>2</sup> )	-	BFT-0.86 DFT-0.85 RFT-0.84	Historical record
[90]	NB-CF, NB-EBF, <b>MLP-CF</b> , MLP-EBF	Romania	Slope angle, convergence index, hydrological soil groups, lithology, land use	Regional (2600 km <sup>2</sup> )	-	NB-CF: 0.929 NB-EBF: 0.884 MLP-CF: 0.932 MLP-EBF: 0.912	Orthophotomaps and field survey
[32]	<b>LMT</b> , KLR, RBFC, NBM	Vietnam	-	-	-	LMT: 0.988; KLR: 0.985; RBFC: 0.984; NBM: 0.983	Aerial photographs, satellite images, and field surveys
[20]	<b>FR</b> , WoE	Romania	No ranking	Regional (340 km <sup>2</sup> )	-	-	Orthophotomaps
[70]	<b>AHP</b>	China	-	National	-	-	-
[26]	<b>CNN</b> , RNN	Iran	Slope degree, altitude, plan curvature, proximity to rivers, lithology	Regional (12,000 km <sup>2</sup> )	30 × 30 m	-	Google Earth images and historical data
[91]	<b>AHP</b>	Iraq	No ranking	Regional (2098 km <sup>2</sup> )	30 × 30 m	-	-
[92]	<b>ANFIS-CF</b> , ANFIS-WOE, ANFIS-AHP	Romania	Slope, distance from river, LULC, lithology, elevation	Regional (4456 km <sup>2</sup> )	-	ANFIS-CF: 0.947 ANFIS-WOE: 0.932 ANFIS-AHP: 0.930	Historical record
[25]	DNN-AHP, <b>DNN-FR</b>	Romania	Land use, profile curvature, hydrological soil group, lithology, slope angle	Regional (2600 km <sup>2</sup> )	30 × 30 m	DNN-AHP: 0.979 DNN-FR: 0.957	Google Earth images and field survey data
[30]	<b>HFPS-RSTree</b> , SVM, RF, C4.5 Dt, LMT	Vietnam	Elevation, slope, aspect, plan curvature, and profile curvature	Regional (1435 km <sup>2</sup> )	30 × 30 m	HFPS-RSTree: 0.967	Sentinel-1 C band images

Table A1. Cont.

References	Model Used (Best Model in Bold)	Study Area	Top 5 Predictors Reported (in No Order)	Implementation Scale	Resolution of the Map Generated	Performance of Models (Based on AUC)	Data against Which the Model Are Validated
[66]	FR, MLP, <b>MLP-FR</b>	Romania	Slope, elevation above channel (EaC), distance from rivers (DfR), plan curvature (PLC), Topographic Wetness Index (TWI)	Regional (5264 km <sup>2</sup> )	25 × 25 m	MLP-FR: 0.986	Satellite imagery and from the RUSLE
[27]	<b>RF</b> , BRT, XGBoost, CART	Romania	Slope, LS factor, TWI, Pasture, HGS	Regional (340 km <sup>2</sup> )	-	RF model: 0.956, BRT: 0.899, XGBoost: 0.892, CART: 0.868	Google Earth aerial imagery
[93]	AHP-FR	Pakistan	Distance from the river, drainage density, slope, elevation, and rainfall.	Regional (14,850 km <sup>2</sup> )	12.5 × 12.5 m	AHP-FR: 0.81	Historical record
[94]	DLNN-FR, <b>DLNN-WOE</b> , ADT-FR, ADT-WOE, WOE, FR), DLNN, ADT	Romania	Slope, profile curvature, land use, Topographic Position Index (TPI), Topographic Wetness Index (TWI)	Regional (340 km <sup>2</sup> )	-	DLNN-FR: 0.942, DLNN-WOE: 0.96, ADT-FR: 0.919, ADT-WOE: 0.94	Google Earth images
[95]	AHP	Egypt	Elevation, slope, lithology, topographic wetness index, distance from the stream	Regional (2900 km <sup>2</sup> )	-	NA	-
[96]	<b>SVR-GOA</b> , SVR-PSO, SVR	India	No ranking	Regional (364.9 km <sup>2</sup> )	-	SVR-GOA: 0.951, SVR-PSO: 0.948, SVR: 0.911	Historical record
[75]	<b>GA-BN-NN</b> ; MLP-BP; GA-MLP; SFLA-MLP	Iran	Elevation, slope angle, the topographic wetness index (TWI), distance to river, drainage density	Regional (4014 km <sup>2</sup> )	30 × 30 m	GA-BN-NN-0.966, MLP-BP-0.908, GA-MLP-0.888, SFLA-MLP-0.941	Aerial photograph, Field survey, and report
[67]	CF. LR, <b>CF-LR</b>	China	6 h precipitation (H6_100) within a 100-year return period, 24 h precipitation (H24_100) within a 100-year return period, annual rainfall, population density, and economic density.	National (120,000 km <sup>2</sup> )	30 × 30 m	CF-LR: 0.86	Historical record
[68]	ANN, DLNN, <b>PSO</b>	India	Aspect, elevation, slope, plan curvature, profile curvature	Regional (465 km <sup>2</sup> )	-	ANN: 0.914, DLNN: 0.920, PSO: 0.942	Historical records, satellite images, and aerial photographs,
[97]	BRT, CART, NBT	UAE	No ranking	Regional (11,871 km <sup>2</sup> )	-	NA	Google Earth application and local reports of newspapers

Table A1. Cont.

References	Model Used (Best Model in Bold)	Study Area	Top 5 Predictors Reported (in No Order)	Implementation Scale	Resolution of the Map Generated	Performance of Models (Based on AUC)	Data against Which the Model Are Validated
[98]	QPSO-CDTree;	Vietnam	Slope, elevation, curvature, topographic wetness index, LULC	Regional (629 km <sup>2</sup> )	30 × 30 m	QPSO-CDTree: 0.949	Past record inventory database
[99]	Geomorphic approach	Pakistan	Geomorphic ranking	Regional (391 km <sup>2</sup> )	-	-	Historical record
[31]	REPT, <b>Decorate-REPT</b> , AdaBoostM1-REPT, Bagging-REPT, and MultiBoostAB-REPT	Vietnam	No ranking	Regional (4662.5 km <sup>2</sup> )	-	Decorate-REPT: 0.988 AdaBoostM1-REPT: 0.983 Bagging-REPT: 0.960 MultiBoostAB-REPT: 0.939	Field survey
[100]	GIS Matrix Method	Bosnia and Herzegovina	No ranking	Regional (6289.19 km <sup>2</sup> )	-	NA	Field survey
[77]	<b>DLNN-AHP</b> , NB-AHP, MLP-AHP, FAHP	Romania	Slope, LULC, convergence index, hydrological soil group, TPI	Regional (363 km <sup>2</sup> )	-	DLNN-AHP: 0.971 NB-AHP: 0.945 MLP-AHP: 0.888 FAHP: 0.836	Aerial imagery from Google Earth
[101]	SVM, CART, CNN, SVM-FMV, CART-FMV, CNN-FMV	China	Altitude, topographic wetness index (TWI), maximum three-day precipitation (M3DP), land cover, soil texture	Regional (90,016 km <sup>2</sup> )	1 km × 1 km	SVM-FMV: 0.915 CART-FMV: 0.915 CNN-FMV: 0.935	Historical record
[102]	AHP	Bangladesh	slope, rainfall, land use land cover, drainage density, digital elevation model	Regional (8590 km <sup>2</sup> )	-	NA	Historical record
[103]	<b>RF</b> , LightGBM, CatBoost	Egypt	TRI, TWI, DEM, slope, distance to river	Regional (138 km <sup>2</sup> )	-	RF: 0.99 LightGBM: 0.98 CatBoost: 0.97	Field surveys and records of historical flood events
[104]	FR, <b>FR-AHP</b>	Malaysia	No ranking	-	-	FR: 0.90 FR-AHP: 0.90	Field visit and Google Earth Pro
[105]	LR, <b>LR-SVM-MLP</b> , SVM, MLP	Pakistan	Distance from river, TWI, curvature, SPI, slope	-	30 × 30 m	LR: 0.978 SVM: 0.968 MLP: 0.985 LR-SVM-MLP: 0.99	
[106]	SI-LR, SI-KNN, SI-RF, <b>SI-XGB</b>	Malaysia	Elevation, distance from river, lithology, river density, rainfall	-	-	SI-LR: 0.977 SI-KNN: 0.98 SI-RF: 0.995 SI-XGB: 0.997	Historical record

Table A1. Cont.

References	Model Used (Best Model in Bold)	Study Area	Top 5 Predictors Reported (in No Order)	Implementation Scale	Resolution of the Map Generated	Performance of Models (Based on AUC)	Data against Which the Model Are Validated
[107]	CNN, LR, KNN	Pakistan	Slope, distance to river, TWI, elevation, distance to road	Regional (1586 km <sup>2</sup> )	12.5 × 12.5 m	CNN: 0.98 LR: 0.97 KNN: 0.95	Historical report
[108]	-	Egypt	Hydro morphometric parameters	Regional (61,000 km <sup>2</sup> )	-	-	-
[109]	FR, FR-SVR, <b>FR-SVR-GWO</b> , FR-SVR-WOA	Iran	No ranking	Regional (17,953 km <sup>2</sup> )	-	FR: 0.86 FR-SVR: 0.83 FR-SVR-GWO: 0.88 FR-SVR-WOA: 0.87	Field survey and historical report
[69]	SVM, LR, Ensemble	Multi-country	No ranking	National (50,640,400 km <sup>2</sup> )	11.1 × 11.1 km	SVM: 0.932 LR: 0.933 Ensemble: 0.934	International Disaster Database (EM-DAT) and the Global Active Archive of Large Flood Events.
[110]	AHP, FR, AHP-FR	Turkey	No ranking	Regional (13,108 km <sup>2</sup> )	-	AHP: 0.965 FR: 0.989 AHP-FR: 0.992	News sources and satellite images
[111]	SE-RF, <b>SE-ANN</b>	Greece	Lithology, LULC, slope, elevation, TWI	Regional (1200 km <sup>2</sup> )	25 × 25 m	SE-RF: 0.87 SE:ANN: 0.773	Field survey and past record
[11]	AHP, F-AHP, ANP, F-ANP, <b>Adaboost</b>	Iran	Runoff, distance from stream, slope, LULC, geology	Regional (11,888 km <sup>2</sup> )	-	AHP: 0.779 F-AHP: 0.750 ANP: 0.850 F-ANP: 0.843 Adaboost: 0.864	Field survey and historical report

## References

- Messner, F.; Meyer, V. Flood damage, vulnerability and risk perception—challenges for flood damage research. In *Flood Risk Management: Hazards, Vulnerability and Mitigation Measures*; Springer: Berlin/Heidelberg, Germany, 2006; pp. 149–167.
- Nachappa, T.G.; Piralilou, S.T.; Gholamnia, K.; Ghorbanzadeh, O.; Rahmati, O.; Blaschke, T. Flood susceptibility mapping with machine learning, multi-criteria decision analysis and ensemble using Dempster Shafer Theory. *J. Hydrol.* **2020**, *590*, 125275. [[CrossRef](#)]
- Iliadis, C.; Galiatsatou, P.; Glenis, V.; Prinos, P.; Kilsby, C. Urban Flood Modelling under Extreme Rainfall Conditions for Building-Level Flood Exposure Analysis. *Hydrology* **2023**, *10*, 172. [[CrossRef](#)]
- Wahlstrom, M.; Guha-Sapir, D. *The Human Cost of Weather-Related Disasters 1995–2015*; UNISDR: Geneva, Switzerland, 2015.
- Avashia, V.; Garg, A. Implications of land use transitions and climate change on local flooding in urban areas: An assessment of 42 Indian cities. *Land Use Policy* **2020**, *95*, 104571. [[CrossRef](#)]
- Hinge, G.; Hamouda, M.A.; Long, D.; Mohamed, M.M. Hydrologic utility of satellite precipitation products in flood Prediction: A meta-data analysis and lessons learnt. *J. Hydrol.* **2022**, *612*, 128103. [[CrossRef](#)]
- Bui, D.T.; Hoang, N.-D.; Pham, T.-D.; Ngo, P.-T.T.; Hoa, P.V.; Minh, N.Q.; Tran, X.-T.; Samui, P. A new intelligence approach based on GIS-based Multivariate Adaptive Regression Splines and metaheuristic optimization for predicting flash flood susceptible areas at high-frequency tropical typhoon area. *J. Hydrol.* **2019**, *575*, 314–326.
- Cao, C.; Xu, P.; Wang, Y.; Chen, J.; Zheng, L.; Niu, C. Flash flood hazard susceptibility mapping using frequency ratio and statistical index methods in coalmine subsidence areas. *Sustainability* **2016**, *8*, 948. [[CrossRef](#)]
- Ghosh, S.; Saha, S.; Bera, B. Flood susceptibility zonation using advanced ensemble machine learning models within Himalayan foreland basin. *Nat. Hazards Res.* **2022**, *2*, 363–374. [[CrossRef](#)]
- Costache, R.; Arabameri, A.; Moayed, H.; Pham, Q.B.; Santosh, M.; Nguyen, H.; Pandey, M.; Pham, B.T. Flash-flood potential index estimation using fuzzy logic combined with deep learning neural network, naïve Bayes, XGBoost and classification and regression tree. *Geocarto Int.* **2021**, *37*, 6780–6807. [[CrossRef](#)]
- Rezaie-Balf, M.; Ghaemi, A.; Jun, C.S.; Band, S.; Bateni, S.M. Towards an integrative, spatially-explicit modeling for flash floods susceptibility mapping based on remote sensing and flood inventory data in Southern Caspian Sea Littoral, Iran. *Geocarto Int.* **2022**, *37*, 12638–12668. [[CrossRef](#)]
- David, A.; Schmalz, B. Flood hazard analysis in small catchments: Comparison of hydrological and hydrodynamic approaches by the use of direct rainfall. *J. Flood Risk Manag.* **2020**, *13*, e12639. [[CrossRef](#)]
- Jong, P.; van den Brink, M. Between tradition and innovation: Developing Flood Risk Management Plans in the Netherlands. *J. Flood Risk Manag.* **2017**, *10*, 155–163. [[CrossRef](#)]
- Grillakis, M.G.; Tsanis, I.K.; Koutroulis, A.G. Application of the HBV hydrological model in a flash flood case in Slovenia. *Nat. Hazards Earth Syst. Sci.* **2010**, *10*, 2713–2725. [[CrossRef](#)]
- Hamouda, M.A.; Hinge, G.; Yemane, H.S.; Al Mosteka, H.; Makki, M.; Mohamed, M.M. Reliability of GPM IMERG Satellite Precipitation Data for Modelling Flash Flood Events in Selected Watersheds in the UAE. *Remote Sens.* **2023**, *15*, 3991. [[CrossRef](#)]
- Glenis, V.; Kutija, V.; Kilsby, C.G. A fully hydrodynamic urban flood modelling system representing buildings, green space and interventions. *Environ. Model. Softw.* **2018**, *109*, 272–292. [[CrossRef](#)]
- Teng, J.; Jakeman, A.J.; Vaze, J.; Croke, B.F.W.; Dutta, D.; Kim, S. Flood inundation modelling: A review of methods, recent advances and uncertainty analysis. *Environ. Model. Softw.* **2017**, *90*, 201–216. [[CrossRef](#)]
- Bellos, V.; Tsakiris, G. A hybrid method for flood simulation in small catchments combining hydrodynamic and hydrological techniques. *J. Hydrol.* **2016**, *540*, 331–339. [[CrossRef](#)]
- Willis, T.; Wright, N.; Sleigh, A. Systematic analysis of uncertainty in 2D flood inundation models. *Environ. Model. Softw.* **2019**, *122*, 104520. [[CrossRef](#)]
- Costache, R.; Zaharia, L. Flash-flood potential assessment and mapping by integrating the weights-of-evidence and frequency ratio statistical methods in GIS environment—case study: Bâsca Chiojdului River catchment (Romania). *J. Earth Syst. Sci.* **2017**, *126*, 59. [[CrossRef](#)]
- Zaharia, L.; Costache, R.; Prăvălie, R.; Minea, G. Assessment and mapping of flood potential in the Slănic catchment in Romania. *J. Earth Syst. Sci.* **2015**, *124*, 1311–1324. [[CrossRef](#)]
- Costache, R. Flash-flood Potential Index mapping using weights of evidence, decision Trees models and their novel hybrid integration. *Stoch. Environ. Res. Risk Assess.* **2019**, *33*, 1375–1402. [[CrossRef](#)]
- Koem, C.; Tantane, S. Flash flood hazard mapping based on AHP with GIS and satellite information in Kampong Speu Province, Cambodia. *Int. J. Disaster Resil. Built Environ.* **2020**, *12*, 457–470. [[CrossRef](#)]
- Radwan, F.; Alazba, A.A.; Mossad, A. Flood risk assessment and mapping using AHP in arid and semiarid regions. *Acta Geophys.* **2019**, *67*, 215–229. [[CrossRef](#)]
- Costache, R.; Ngo, P.T.T.; Bui, D.T. Novel ensembles of deep learning neural network and statistical learning for flash-flood susceptibility mapping. *Water* **2020**, *12*, 1549. [[CrossRef](#)]
- Panahi, M.; Jaafari, A.; Shirzadi, A.; Shahabi, H.; Rahmati, O.; Omidvar, E.; Lee, S.; Bui, D.T. Deep learning neural networks for spatially explicit prediction of flash flood probability. *Geosci. Front.* **2021**, *12*, 101076. [[CrossRef](#)]
- Abedi, R.; Costache, R.; Shafizadeh-Moghadam, H.; Pham, Q.B. Flash-flood susceptibility mapping based on XGBoost, random forest and boosted regression trees. *Geocarto Int.* **2021**, *37*, 5479–5496. [[CrossRef](#)]

28. Muñoz, P.; Orellana-Alvear, J.; Willems, P.; Célleri, R. Flash-flood forecasting in an Andean mountain catchment—Development of a step-wise methodology based on the random forest algorithm. *Water* **2018**, *10*, 1519. [[CrossRef](#)]
29. Chen, W.; Hong, H.; Li, S.; Shahabi, H.; Wang, Y.; Wang, X.; Ahmad, B. Bin Flood susceptibility modelling using novel hybrid approach of reduced-error pruning trees with bagging and random subspace ensembles. *J. Hydrol.* **2019**, *575*, 864–873. [[CrossRef](#)]
30. Nhu, V.-H.; Thi Ngo, P.-T.; Pham, T.D.; Dou, J.; Song, X.; Hoang, N.-D.; Tran, D.A.; Cao, D.P.; Aydilek, I.B.; Amiri, M. A new hybrid firefly–PSO optimized random subspace tree intelligence for torrential rainfall-induced flash flood susceptible mapping. *Remote Sens.* **2020**, *12*, 2688. [[CrossRef](#)]
31. Ha, H.; Luu, C.; Bui, Q.D.; Pham, D.-H.; Hoang, T.; Nguyen, V.-P.; Vu, M.T.; Pham, B.T. Flash flood susceptibility prediction mapping for a road network using hybrid machine learning models. *Nat. Hazards* **2021**, *109*, 1247–1270. [[CrossRef](#)]
32. Pham, B.T.; Van Phong, T.; Nguyen, H.D.; Qi, C.; Al-Ansari, N.; Amini, A.; Ho, L.S.; Tuyen, T.T.; Yen, H.P.H.; Ly, H.-B. A comparative study of kernel logistic regression, radial basis function classifier, multinomial naïve bayes, and logistic model tree for flash flood susceptibility mapping. *Water* **2020**, *12*, 239. [[CrossRef](#)]
33. Hapuarachchi, H.A.P.; Wang, Q.J.; Pagano, T.C. A review of advances in flash flood forecasting. *Hydrol. Process.* **2011**, *25*, 2771–2784. [[CrossRef](#)]
34. Saleh, A.; Yuzir, A.; Abustan, I. Flash flood susceptibility modelling: A review. In Proceedings of the 3rd National Conference on Wind & Earthquake Engineering and International Seminar On Sustainable Construction Engineering, Kuala Lumpur, Malaysia, 12–13 July 2019; IOP Publishing: Bristol, UK, 2020; Volume 712, p. 12005.
35. Zanchetta, A.D.L.; Coulibaly, P. Recent advances in real-time pluvial flash flood forecasting. *Water* **2020**, *12*, 570. [[CrossRef](#)]
36. Liu, C.; Guo, L.; Ye, L.; Zhang, S.; Zhao, Y.; Song, T. A review of advances in China’s flash flood early-warning system. *Nat. Hazards* **2018**, *92*, 619–634. [[CrossRef](#)]
37. Hinge, G.; Mohamed, M.M.; Long, D.; Hamouda, M.A. Meta-Analysis in Using Satellite Precipitation Products for Drought Monitoring: Lessons Learnt and Way Forward. *Remote Sens.* **2021**, *13*, 4353. [[CrossRef](#)]
38. Islam, A.; Hassini, S.; El-Dakhkhni, W. A systematic bibliometric review of optimization and resilience within low impact development stormwater management practices. *J. Hydrol.* **2021**, *599*, 126457. [[CrossRef](#)]
39. Maditati, D.R.; Munim, Z.H.; Schramm, H.-J.; Kummer, S. A review of green supply chain management: From bibliometric analysis to a conceptual framework and future research directions. *Resour. Conserv. Recycl.* **2018**, *139*, 150–162. [[CrossRef](#)]
40. Chiu, W.-T.; Ho, Y.-S. Bibliometric analysis of tsunami research. *Scientometrics* **2007**, *73*, 3–17. [[CrossRef](#)]
41. Dordi, T.; Henstra, D.; Thistlethwaite, J. Flood risk management and governance: A bibliometric review of the literature. *J. Flood Risk Manag.* **2022**, *15*, e12797. [[CrossRef](#)]
42. Durán-Sánchez, A.; Álvarez-García, J.; González-Vázquez, E.; Río-Rama, D.; de la Cruz, M. Wastewater management: Bibliometric analysis of scientific literature. *Water* **2020**, *12*, 2963. [[CrossRef](#)]
43. Wu, J.; Wu, X.; Zhang, J. Development trend and frontier of stormwater management (1980–2019): A bibliometric overview based on CiteSpace. *Water* **2019**, *11*, 1908. [[CrossRef](#)]
44. Garfield, E.; Paris, S.; Stock, W.G. HistCiteTM: A software tool for informetric analysis of citation linkage. *Inf. Wiss. Prax.* **2006**, *57*, 391.
45. Van Eck, N.; Waltman, L. Software survey: VOSviewer, a computer program for bibliometric mapping. *Scientometrics* **2010**, *84*, 523–538. [[CrossRef](#)]
46. Wehling, P.; LaBudde, R.A.; Brunelle, S.L.; Nelson, M.T. Probability of detection (POD) as a statistical model for the validation of qualitative methods. *J. AOAC Int.* **2011**, *94*, 335–347. [[CrossRef](#)] [[PubMed](#)]
47. Plataridis, K.; Mallios, Z. Flood susceptibility mapping using hybrid models optimized with Artificial Bee Colony. *J. Hydrol.* **2023**, *624*, 129961. [[CrossRef](#)]
48. Ling, C.X.; Huang, J.; Zhang, H. AUC: A statistically consistent and more discriminating measure than accuracy. In Proceedings of the Eighteenth International Joint Conference on Artificial Intelligence, Acapulco, Mexico, 9–15 August 2003; Volume 3, pp. 519–524.
49. Bentivoglio, R.; Isufi, E.; Jonkman, S.N.; Taormina, R. Deep Learning Methods for Flood Mapping: A Review of Existing Applications and Future Research Directions. *Hydrol. Earth Syst. Sci.* **2021**, *26*, 4345–4378. [[CrossRef](#)]
50. De Moel, H.; Jongman, B.; Kreibich, H.; Merz, B.; Penning-Rowsell, E.; Ward, P.J. Flood risk assessments at different spatial scales. *Mitig. Adapt. Strateg. Glob. Chang.* **2015**, *20*, 865–890. [[CrossRef](#)] [[PubMed](#)]
51. Khosravi, K.; Pham, B.T.; Chapi, K.; Shirzadi, A.; Shahabi, H.; Revhaug, I.; Prakash, I.; Bui, D.T. A comparative assessment of decision trees algorithms for flash flood susceptibility modeling at Haraz watershed, northern Iran. *Sci. Total Environ.* **2018**, *627*, 744–755. [[CrossRef](#)] [[PubMed](#)]
52. Zhao, G.; Pang, B.; Xu, Z.; Yue, J.; Tu, T. Mapping flood susceptibility in mountainous areas on a national scale in China. *Sci. Total Environ.* **2018**, *615*, 1133–1142. [[CrossRef](#)]
53. Bui, D.T.; Hoang, N.-D.; Martínez-Álvarez, F.; Ngo, P.-T.T.; Hoa, P.V.; Pham, T.D.; Samui, P.; Costache, R. A novel deep learning neural network approach for predicting flash flood susceptibility: A case study at a high frequency tropical storm area. *Sci. Total Environ.* **2020**, *701*, 134413.
54. Hosseini, F.S.; Choubin, B.; Mosavi, A.; Nabipour, N.; Shamshirband, S.; Darabi, H.; Haghghi, A.T. Flash-flood hazard assessment using ensembles and Bayesian-based machine learning models: Application of the simulated annealing feature selection method. *Sci. Total Environ.* **2020**, *711*, 135161. [[CrossRef](#)]

55. Khosravi, K.; Pourghasemi, H.R.; Chapi, K.; Bahri, M. Flash flood susceptibility analysis and its mapping using different bivariate models in Iran: A comparison between Shannon's entropy, statistical index, and weighting factor models. *Environ. Monit. Assess.* **2016**, *188*, 656. [[CrossRef](#)] [[PubMed](#)]
56. Bui, D.T.; Ngo, P.-T.T.; Pham, T.D.; Jaafari, A.; Minh, N.Q.; Hoa, P.V.; Samui, P. A novel hybrid approach based on a swarm intelligence optimized extreme learning machine for flash flood susceptibility mapping. *Catena* **2019**, *179*, 184–196. [[CrossRef](#)]
57. Bui, D.T.; Tsangaratos, P.; Ngo, P.-T.T.; Pham, T.D.; Pham, B.T. Flash flood susceptibility modeling using an optimized fuzzy rule based feature selection technique and tree based ensemble methods. *Sci. Total Environ.* **2019**, *668*, 1038–1054. [[CrossRef](#)] [[PubMed](#)]
58. Islam, A.R.M.T.; Talukdar, S.; Mahato, S.; Kundu, S.; Eibek, K.U.; Pham, Q.B.; Kuriqi, A.; Linh, N.T.T. Flood susceptibility modelling using advanced ensemble machine learning models. *Geosci. Front.* **2021**, *12*, 101075. [[CrossRef](#)]
59. Youssef, A.M.; Pradhan, B.; Sefry, S.A. Flash flood susceptibility assessment in Jeddah city (Kingdom of Saudi Arabia) using bivariate and multivariate statistical models. *Environ. Earth Sci.* **2016**, *75*, 12. [[CrossRef](#)]
60. Mohamed, A.; Razak, A.Z.A.; Abdullah, Z. Most-Cited Research Publications on Educational Leadership and Management: A Bibliometric Analysis. *Int. Online J. Educ. Leadersh.* **2020**, *4*, 33–50.
61. Elkhrachy, I. Flash flood hazard mapping using satellite images and GIS tools: A case study of Najran City, Kingdom of Saudi Arabia (KSA). *Egypt. J. Remote Sens. Space Sci.* **2015**, *18*, 261–278. [[CrossRef](#)]
62. Bandi, A.S.; Meshapam, S.; Deva, P. A geospatial approach to flash flood hazard mapping in the city of Warangal, Telangana, India. *Environ. Socio-Econ. Stud.* **2019**, *7*, 1–13. [[CrossRef](#)]
63. Yoshimoto, S.; Amarnath, G. Applications of satellite-based rainfall estimates in flood inundation modeling—A case study in Mundeni Aru River Basin, Sri Lanka. *Remote Sens.* **2017**, *9*, 998. [[CrossRef](#)]
64. Nair, A.S.; Soman, M.K.; Girish, P.; Karmakar, S.; Indu, J. Evaluating SWOT Water Level Information Using a Large Scale Hydrology Simulator: A Case Study Over India. *Adv. Space Res.* **2022**, *70*, 1362–1374. [[CrossRef](#)]
65. Khosravi, K.; Shahabi, H.; Pham, B.T.; Adamowski, J.; Shirzadi, A.; Pradhan, B.; Dou, J.; Ly, H.-B.; Gróf, G.; Ho, H.L. A comparative assessment of flood susceptibility modeling using multi-criteria decision-making analysis and machine learning methods. *J. Hydrol.* **2019**, *573*, 311–323. [[CrossRef](#)]
66. Popa, M.C.; Peptenatu, D.; Drăghici, C.C.; Diaconu, D.C. Flood hazard mapping using the flood and flash-flood potential index in the Buzău river catchment, Romania. *Water* **2019**, *11*, 2116. [[CrossRef](#)]
67. Cao, Y.; Jia, H.; Xiong, J.; Cheng, W.; Li, K.; Pang, Q.; Yong, Z. Flash Flood Susceptibility Assessment Based on Geodetector, Certainty Factor, and Logistic Regression Analyses in Fujian Province, China. *ISPRS Int. J. Geo-Inf.* **2020**, *9*, 748. [[CrossRef](#)]
68. Chakraborty, R.; Chandra Pal, S.; Rezaie, F.; Arabameri, A.; Lee, S.; Roy, P.; Saha, A.; Chowdhuri, I.; Moayed, H. Flash-flood hazard susceptibility mapping in Kangsabati River Basin, India. *Geocarto Int.* **2021**, *37*, 6713–6735. [[CrossRef](#)]
69. Liu, J.; Wang, J.; Xiong, J.; Cheng, W.; Li, Y.; Cao, Y.; He, Y.; Duan, Y.; He, W.; Yang, G. Assessment of flood susceptibility mapping using support vector machine, logistic regression and their ensemble techniques in the Belt and Road region. *Geocarto Int.* **2022**, *37*, 9817–9846. [[CrossRef](#)]
70. Xiong, J.; Li, J.; Cheng, W.; Wang, N.; Guo, L. A GIS-based support vector machine model for flash flood vulnerability assessment and mapping in China. *ISPRS Int. J. Geo-Inf.* **2019**, *8*, 297. [[CrossRef](#)]
71. Shahabi, H.; Shirzadi, A.; Ronoud, S.; Asadi, S.; Pham, B.T.; Mansouripour, F.; Geertsema, M.; Clague, J.J.; Bui, D.T. Flash flood susceptibility mapping using a novel deep learning model based on deep belief network, back propagation and genetic algorithm. *Geosci. Front.* **2021**, *12*, 101100. [[CrossRef](#)]
72. Zaharia, L.; Costache, R.; Prăvălie, R.; Ioana-Toroimac, G. Mapping flood and flooding potential indices: A methodological approach to identifying areas susceptible to flood and flooding risk. Case study: The Prahova catchment (Romania). *Front. Earth Sci.* **2017**, *11*, 229–247. [[CrossRef](#)]
73. Costache, R.; Bui, D.T. Spatial prediction of flood potential using new ensembles of bivariate statistics and artificial intelligence: A case study at the Putna river catchment of Romania. *Sci. Total Environ.* **2019**, *691*, 1098–1118. [[CrossRef](#)]
74. Ngo, P.-T.T.; Hoang, N.-D.; Pradhan, B.; Nguyen, Q.K.; Tran, X.T.; Nguyen, Q.M.; Nguyen, V.N.; Samui, P.; Tien Bui, D. A novel hybrid swarm optimized multilayer neural network for spatial prediction of flash floods in tropical areas using sentinel-1 SAR imagery and geospatial data. *Sensors* **2018**, *18*, 3704. [[CrossRef](#)]
75. Shirzadi, A.; Asadi, S.; Shahabi, H.; Ronoud, S.; Clague, J.J.; Khosravi, K.; Pham, B.T.; Ahmad, B.B.; Bui, D.T. A novel ensemble learning based on Bayesian Belief Network coupled with an extreme learning machine for flash flood susceptibility mapping. *Eng. Appl. Artif. Intell.* **2020**, *96*, 103971. [[CrossRef](#)]
76. Prasad, P.; Loveson, V.J.; Das, B.; Kotha, M. Novel ensemble machine learning models in flood susceptibility mapping. *Geocarto Int.* **2021**, *37*, 4571–4593. [[CrossRef](#)]
77. Costache, R.; Tin, T.T.; Arabameri, A.; Crăciun, A.; Ajin, R.S.; Costache, I.; Islam, A.R.M.T.; Abba, S.I.; Sahana, M.; Avand, M. Flash-flood hazard using deep learning based on H<sub>2</sub>O R package and fuzzy-multicriteria decision-making analysis. *J. Hydrol.* **2022**, *609*, 127747. [[CrossRef](#)]
78. Tehrany, M.S.; Pradhan, B.; Jebur, M.N. Flood susceptibility mapping using a novel ensemble weights-of-evidence and support vector machine models in GIS. *J. Hydrol.* **2014**, *512*, 332–343. [[CrossRef](#)]
79. Tien Bui, D.; Shirzadi, A.; Shahabi, H.; Chapi, K.; Omidav, E.; Pham, B.T.; Talebpour Asl, D.; Khaledian, H.; Pradhan, B.; Panahi, M. A novel ensemble artificial intelligence approach for gully erosion mapping in a semi-arid watershed (Iran). *Sensors* **2019**, *19*, 2444. [[CrossRef](#)]



80. Janizadeh, S.; Avand, M.; Jaafari, A.; Van Phong, T.; Bayat, M.; Ahmadisharaf, E.; Prakash, I.; Pham, B.T.; Lee, S. Prediction success of machine learning methods for flash flood susceptibility mapping in the Tafresh watershed, Iran. *Sustainability* **2019**, *11*, 5426. [[CrossRef](#)]
81. Costache, R.; Pham, Q.B.; Sharifi, E.; Linh, N.T.T.; Abba, S.I.; Vojtek, M.; Vojteková, J.; Nhi, P.T.T.; Khoi, D.N. Flash-flood susceptibility assessment using multi-criteria decision making and machine learning supported by remote sensing and GIS techniques. *Remote Sens.* **2019**, *12*, 106. [[CrossRef](#)]
82. Bui, Q.-T.; Nguyen, Q.-H.; Nguyen, X.L.; Pham, V.D.; Nguyen, H.D.; Pham, V.-M. Verification of novel integrations of swarm intelligence algorithms into deep learning neural network for flood susceptibility mapping. *J. Hydrol.* **2020**, *581*, 124379. [[CrossRef](#)]
83. Pham, B.T.; Avand, M.; Janizadeh, S.; Van Phong, T.; Al-Ansari, N.; Ho, L.S.; Das, S.; Van Le, H.; Amini, A.; Bozchaloei, S.K. GIS based hybrid computational approaches for flash flood susceptibility assessment. *Water* **2020**, *12*, 683. [[CrossRef](#)]
84. Costache, R. Flash-Flood Potential assessment in the upper and middle sector of Prahova river catchment (Romania). A comparative approach between four hybrid models. *Sci. Total Environ.* **2019**, *659*, 1115–1134. [[CrossRef](#)]
85. Costache, R.; Bui, D.T. Identification of areas prone to flash-flood phenomena using multiple-criteria decision-making, bivariate statistics, machine learning and their ensembles. *Sci. Total Environ.* **2020**, *712*, 136492. [[CrossRef](#)]
86. Band, S.S.; Janizadeh, S.; Chandra Pal, S.; Saha, A.; Chakraborty, R.; Melesse, A.M.; Mosavi, A. Flash flood susceptibility modeling using new approaches of hybrid and ensemble tree-based machine learning algorithms. *Remote Sens.* **2020**, *12*, 3568. [[CrossRef](#)]
87. Costache, R.; Hong, H.; Pham, Q.B. Comparative assessment of the flash-flood potential within small mountain catchments using bivariate statistics and their novel hybrid integration with machine learning models. *Sci. Total Environ.* **2020**, *711*, 134514. [[CrossRef](#)]
88. Arabameri, A.; Saha, S.; Mukherjee, K.; Blaschke, T.; Chen, W.; Ngo, P.T.T.; Band, S.S. Modeling spatial flood using novel ensemble artificial intelligence approaches in northern Iran. *Remote Sens.* **2020**, *12*, 3423. [[CrossRef](#)]
89. Arabameri, A.; Saha, S.; Chen, W.; Roy, J.; Pradhan, B.; Bui, D.T. Flash flood susceptibility modelling using functional tree and hybrid ensemble techniques. *J. Hydrol.* **2020**, *587*, 125007. [[CrossRef](#)]
90. Costache, R.; Hong, H.; Wang, Y. Identification of torrential valleys using GIS and a novel hybrid integration of artificial intelligence, machine learning and bivariate statistics. *Catena* **2019**, *183*, 104179. [[CrossRef](#)]
91. Al-Abadi, A.M.; Shahid, S.; Al-Ali, A.K. A GIS-based integration of catastrophe theory and analytical hierarchy process for mapping flood susceptibility: A case study of Teeb area, Southern Iraq. *Environ. Earth Sci.* **2016**, *75*, 687. [[CrossRef](#)]
92. Costache, R.; Țincu, R.; Elkhrachy, I.; Pham, Q.B.; Popa, M.C.; Diaconu, D.C.; Avand, M.; Costache, I.; Arabameri, A.; Bui, D.T. New neural fuzzy-based machine learning ensemble for enhancing the prediction accuracy of flood susceptibility mapping. *Hydrol. Sci. J.* **2020**, *65*, 2816–2837. [[CrossRef](#)]
93. Waqas, H.; Lu, L.; Tariq, A.; Li, Q.; Baqa, M.F.; Xing, J.; Sajjad, A. Flash flood susceptibility assessment and zonation using an integrating analytic hierarchy process and frequency ratio model for the Chitral District, Khyber Pakhtunkhwa, Pakistan. *Water* **2021**, *13*, 1650. [[CrossRef](#)]
94. Costache, R.; Arabameri, A.; Blaschke, T.; Pham, Q.B.; Pham, B.T.; Pandey, M.; Arora, A.; Linh, N.T.T.; Costache, I. Flash-flood potential mapping using deep learning, alternating decision trees and data provided by remote sensing sensors. *Sensors* **2021**, *21*, 280. [[CrossRef](#)]
95. El-Magd, S.A.A.; Amer, R.A.; Embaby, A. Multi-criteria decision-making for the analysis of flash floods: A case study of Awlad Toq-Sherq, Southeast Sohag, Egypt. *J. Afr. Earth Sci.* **2020**, *162*, 103709. [[CrossRef](#)]
96. Ruidas, D.; Chakraborty, R.; Islam, A.R.M.; Saha, A.; Pal, S.C. A novel hybrid of meta-optimization approach for flash flood-susceptibility assessment in a monsoon-dominated watershed, Eastern India. *Environ. Earth Sci.* **2022**, *81*, 145. [[CrossRef](#)]
97. Elmahdy, S.; Ali, T.; Mohamed, M. Flash Flood Susceptibility modeling and magnitude index using machine learning and geohydrological models: A modified hybrid approach. *Remote Sens.* **2020**, *12*, 2695. [[CrossRef](#)]
98. Ngo, P.-T.T.; Pham, T.D.; Nhu, V.-H.; Le, T.T.; Tran, D.A.; Phan, D.C.; Hoa, P.V.; Amaro-Mellado, J.L.; Bui, D.T. A novel hybrid quantum-PSO and credal decision tree ensemble for tropical cyclone induced flash flood susceptibility mapping with geospatial data. *J. Hydrol.* **2021**, *596*, 125682. [[CrossRef](#)]
99. Mahmood, S.; Rahman, A.-U. Flash flood susceptibility modelling using geomorphometric approach in the Ushairy Basin, eastern Hindu Kush. *J. Earth Syst. Sci.* **2019**, *128*, 43. [[CrossRef](#)]
100. Tošić, R.; Lovrić, N.; Dragičević, S.; Manojlović, S. Assessment of torrential flood susceptibility using GIS matrix method: Case study-VRBAS river basin (B&H). *Carpathian J. Earth Environ. Sci.* **2018**, *13*, 369–382.
101. Liu, J.; Wang, J.; Xiong, J.; Cheng, W.; Sun, H.; Yong, Z.; Wang, N. Hybrid Models Incorporating Bivariate Statistics and Machine Learning Methods for Flash Flood Susceptibility Assessment Based on Remote Sensing Datasets. *Remote Sens.* **2021**, *13*, 4945. [[CrossRef](#)]
102. Haque, M.; Siddika, S.; Sresto, M.A.; Saroar, M.; Shabab, K.R. Geo-spatial Analysis for Flash Flood Susceptibility Mapping in the North-East Haor (Wetland) Region in Bangladesh. *Earth Syst. Environ.* **2021**, *5*, 365–384. [[CrossRef](#)]
103. Saber, M.; Boulmaiz, T.; Guermoui, M.; Abdrabo, K.I.; Kantoush, S.A.; Sumi, T.; Boutaghane, H.; Nohara, D.; Mabrouk, E. Examining LightGBM and CatBoost models for wadi flash flood susceptibility prediction. *Geocarto Int.* **2021**, *37*, 7462–7487. [[CrossRef](#)]
104. Saleh, A.; Yuzir, A.; Sabtu, N. Flash flood susceptibility mapping of sungai pinang catchment using frequency ratio. *Sains Malays.* **2022**, *51*, 51–65. [[CrossRef](#)]

105. Yaseen, A.; Lu, J.; Chen, X. Flood susceptibility mapping in an arid region of Pakistan through ensemble machine learning model. *Stoch. Environ. Res. Risk Assess.* **2022**, *36*, 3041–3061. [[CrossRef](#)]
106. Saleh, A.; Yuzir, A.; Sabtu, N.; Abujayyab, S.K.M.; Bunmi, M.R.; Pham, Q.B. Flash flood susceptibility mapping in urban area using genetic algorithm and ensemble method. *Geocarto Int.* **2022**, *37*, 10199–10228. [[CrossRef](#)]
107. Ullah, K.; Wang, Y.; Fang, Z.; Wang, L.; Rahman, M. Multi-hazard susceptibility mapping based on Convolutional Neural Networks. *Geosci. Front.* **2022**, *13*, 101425. [[CrossRef](#)]
108. El-Rawy, M.; Elsadek, W.M.; De Smedt, F. Flash Flood Susceptibility Mapping in Sinai, Egypt Using Hydromorphic Data, Principal Component Analysis and Logistic Regression. *Water* **2022**, *14*, 2434. [[CrossRef](#)]
109. Rezaie, F.; Panahi, M.; Bateni, S.M.; Jun, C.; Neale, C.M.U.; Lee, S. Novel hybrid models by coupling support vector regression (SVR) with meta-heuristic algorithms (WOA and GWO) for flood susceptibility mapping. *Nat. Hazards* **2022**, *114*, 1247–1283. [[CrossRef](#)]
110. Yilmaz, O.S. Flood hazard susceptibility areas mapping using Analytical Hierarchical Process (AHP), Frequency Ratio (FR) and AHP-FR ensemble based on Geographic Information Systems (GIS): A case study for Kastamonu, Türkiye. *Acta Geophys.* **2022**, *70*, 2747–2769. [[CrossRef](#)]
111. Ilija, I.; Tsangaratos, P.; Tzampoglou, P.; Chen, W.; Hong, H. Flash flood susceptibility mapping using stacking ensemble machine learning models. *Geocarto Int.* **2022**, *37*, 15010–15036. [[CrossRef](#)]

**Disclaimer/Publisher’s Note:** The statements, opinions and data contained in all publications are solely those of the individual author(s) and contributor(s) and not of MDPI and/or the editor(s). MDPI and/or the editor(s) disclaim responsibility for any injury to people or property resulting from any ideas, methods, instructions or products referred to in the content.